

# Stability and stabilization of semilinear single-track vehicle models with distributed tire friction dynamics via singular perturbation analysis

Luigi Romano<sup>\*a,b,c</sup>, Ole Morten Aamo<sup>b</sup>, Miroslav Krstić<sup>c</sup>, Jan Aslund<sup>a</sup>, and Erik Frisk<sup>a</sup>

<sup>a</sup>Department of Electrical Engineering, Linköping University, SE-581 83 Linköping, Sweden

<sup>b</sup>Department of Engineering Cybernetics, Norwegian University of Science and Technology, O. S. Bragstads plass 2, NO-7034, Trondheim, Norway

<sup>c</sup>Department of Mechanical and Aerospace Engineering, University of California San Diego, La Jolla, CA, 92093, USA

**Abstract.** This paper investigates the stability and stabilization of semilinear single-track vehicle models with distributed tire friction dynamics, modeled as interconnections of ordinary differential equations (ODEs) and hyperbolic partial differential equations (PDEs). Motivated by the long-standing practice of neglecting transient tire dynamics in vehicle modeling and control, a rigorous justification is provided for such simplifications using singular perturbation theory. A perturbation parameter, defined as the ratio between a characteristic rolling contact length and the vehicle's longitudinal speed, is introduced to formalize the time-scale separation between rigid-body motion and tire dynamics. For sufficiently small values of this parameter, it is demonstrated that standard finite-dimensional techniques can be applied to analyze the local stability of equilibria and to design stabilizing controllers. Both state-feedback and output-feedback designs are considered, under standard stabilizability and detectability assumptions. Whilst the proposed controllers follow classical approaches, the novelty of the work lies in establishing the first mathematical framework that rigorously connects distributed tire models with conventional vehicle dynamics. The results reconcile decades of empirical findings with a formal theoretical foundation and open new perspectives for the analysis and control of ODE-PDE systems with distributed friction in automotive applications.

**Keywords:** Vehicle dynamics; distributed friction models; distributed parameter systems; hyperbolic ODE-PDE systems; semilinear systems; singular perturbation theory

## 1 Introduction

The analysis and control of road vehicles have long been central topics in both automotive and control engineering. A key aspect of these studies is the modeling of tire-road interaction, which fundamentally determines the stability, handling, and safety of road vehicles. In most of the classical literature, the transient dynamics of tires are neglected, and tires are instead modeled as static nonlinearities that map slip conditions into forces (Pacejka 2012; Guiggiani 2023; Romano 2022). This modeling choice has been extremely influential: it simplifies analysis, enables the adoption of low-order vehicle models, and underpins many of the widely adopted techniques for stability analysis, control design, and observer synthesis (Sharifzadeh, Akbari, et al. 2016; Sharifzadeh, Senatore, et al. 2019; Shao et al. 2016; Shao et al. 2019; Guo et al. 2021; Lenzo, Zanchetta, and Sorniotti 2020; Li et al. 2022; Tanelli, Astolfi, and Savaresi 2008; Talbot, Brown, and Gerdes 2023; Du, Zhang, and Dong 2010; Zhou et al. 2018; Nam, Fujimoto, and Hori 2012) based on static tire models. Such models continue to serve as the backbone for advanced driver assistance systems, observer design for lateral dynamics, and even the development of automated driving technologies.

As explained in Takács and Stépán (2013), the informal justification behind this simplification lies in a perceived separation of time scales: vehicle rigid-body dynamics evolve

relatively slowly compared to the fast rolling contact phenomena taking place inside the tire patch. Building on this consideration, it becomes reasonable to treat tire forces as quasi-stationary functions of slip (Pacejka 2012; Guiggiani 2023), thereby enabling the application of well-established finite-dimensional control methods. The validity of this approximation appears evident if not pleonastic: a vast corpus of literature reports numerical validations, experimental verifications, and successful estimator (Sharifzadeh, Akbari, et al. 2016; Sharifzadeh, Senatore, et al. 2019; Shao et al. 2016; Shao et al. 2019) and controller implementations (Guo et al. 2021; Lenzo, Zanchetta, and Sorniotti 2020; Li et al. 2022; Tanelli, Astolfi, and Savaresi 2008; Talbot, Brown, and Gerdes 2023; Du, Zhang, and Dong 2010; Zhou et al. 2018; Nam, Fujimoto, and Hori 2012) based on static tire models. Such models continue to serve as the backbone for advanced driver assistance systems, observer design for lateral dynamics, and even the development of automated driving technologies.

Despite this practical success, the lack of a rigorous theoretical foundation for neglecting tire transients has remained a notable gap. The separation-of-time-scales argument, whilst intuitively appealing, has not been systematically formalized in the context of stability and control of vehicle models. The omission becomes especially rele-

<sup>\*</sup>Corresponding author. Email: luigi.romano@liu.se.

tant when operating conditions depart from those for which static models are most accurate. For instance, recent research by Takács and Stépán (2013), Takács and Stépán (2012), Takács, Orosz, and Stépán (2009), Takács, Stépán, and Hogan (2008), Beregi, Takács, and Stépán (2016), Beregi, Takács, and Gyebroszki (2019), and Romano, Aamo, Åslund, et al. (2024) has highlighted differences between predictions obtained using conventional static tire models and those incorporating transient, distributed tire dynamics. These discrepancies are particularly pronounced at low rolling speeds, where the time scales of tire deformation and rigid-body motion are no longer well separated. Under these conditions, transient tire behavior manifest in non-trivial dynamical effects, including oscillatory instabilities and micro-shimmy phenomena, that static models cannot capture.

To address these limitations, distributed tire models expressed in terms of semilinear hyperbolic partial differential equations (PDEs) have been proposed in Romano (2022), Canudas-de-Wit and Tsotras (1999), Canudas-de-Wit, Tsotras, and Velenis (2003), Velenis et al. (2005), Deur (2001), Deur, Asgari, and Hrovat (2004), and Deur, Ivanović, and Troulis (2005). These models capture the spatiotemporal evolution of frictional stresses inside the contact patch and naturally account for the nonstationary generation of longitudinal and lateral forces. Incorporating such descriptions into complete vehicle models yields ODE-PDE interconnections, where the vehicle's rigid-body states interact with the distributed dynamics of the tire-road interface (Romano, Aamo, Åslund, et al. 2026b). Whilst this modeling framework is more realistic and can reproduce subtle dynamical phenomena, it introduces new analytical and control-theoretic challenges: questions of well-posedness, stability, and controller synthesis would involve infinite-dimensional systems (Weiss and Curtain 1997; Curtain and Zwart 2020), with the established toolbox of finite-dimensional methods being not directly applicable.

Over the past two decades, significant progress has been made in the control of PDE and ODE-PDE interconnections, with powerful techniques developed in areas such as chemical process control, flexible structures, and flow dynamics (Bastin and Coron 2016; Krstić and Smyshlyaev 2008; Vazquez and Krstić 2007; Anfinsen and Aamo 2019). Notably, singular perturbation methods, typically restricted to ODEs, have been extended to analyze and stabilize hyperbolic PDE and ODE-PDE systems with multiple time scales in Vazquez and Krstić (2006), Tang, Prieur, and Girard (2015), Tang and Mazanti (2017), and Cerpa and Prieur (2017). However, the application of such methods to vehicle dynamics has been limited, and a systematic connection between distributed tire models and standard vehicle dynamics theory has been missing.

The present paper aims to close this gap by providing the first rigorous justification for the use of conventional finite-dimensional tools in vehicle stability and control, when applied to models that include distributed tire dynamics. Specifically, this work focuses on simple semilinear single-track vehicle models with PDE-based representations of tire friction dynamics. Leveraging singular perturbation analysis, it demonstrates that, for sufficiently small values of a

perturbation parameter – defined as the ratio between a characteristic length scale of the rolling contact process and the vehicle's longitudinal speed – the semilinear ODE-PDE interconnection can be approximated by a reduced finite-dimensional subsystem. In this regime, classical tools of nonlinear stability analysis and controller design can be reliably applied. Importantly, this result formalizes the heuristic justification for neglecting transient tire dynamics at sufficiently high velocities, whilst simultaneously clarifying the conditions under which such simplifications fail. Building on this foundation, the stabilization problem is also addressed. Both state-feedback and output-feedback controllers are synthesized, relying on standard stabilizability and detectability assumptions. Although the proposed control strategies themselves are not new (being, in fact, the simplest known), the contribution of this work lies in establishing that their use is theoretically justified for ODE-PDE vehicle models under explicit conditions. In this way, the paper reconciles decades of empirical and simulation-based validation of static tire models with a rigorous mathematical framework.

The contributions of this paper are twofold. First, it provides novel singular-perturbation-based stability results for semilinear vehicle models with distributed tire dynamics, thereby extending the theoretical understanding of vehicle stability into the infinite-dimensional setting. Second, it demonstrates that widely adopted finite-dimensional design methods for vehicle control and observation can be systematically justified when tire dynamics evolve on faster time scales than the rigid-body motion. Albeit derived using simplified ODE-PDE vehicle models, these contributions not only advance the fundamental theory of vehicle dynamics but also open new avenues for the design of controllers and observers for ODE-PDE systems with distributed friction, which may ultimately improve the safety and robustness of future intelligent vehicles.

The remainder of the paper is organized as follows. Section 2 introduces the family of semilinear single-track vehicle models with distributed tire friction dynamics considered throughout the manuscript, and postulates some structural assumptions. A stability analysis is then conducted in Section 3 using singular perturbation theory, first by isolating the reduced ODE and boundary-layer PDE subsystems, and then by deriving local stability results for sufficiently small perturbation parameters. Section 4 addresses the stabilization problem, presenting state-feedback and output-feedback designs and extending their validity through singular perturbation arguments. Numerical simulations are discussed in Section 5. Finally, Section 6 concludes the paper with remarks on implications for vehicle dynamics and directions for future research.

## Notation

In this paper,  $\mathbb{R}$  denotes the set of real numbers;  $\mathbb{R}_{>0}$  and  $\mathbb{R}_{\geq 0}$  indicate the set of positive real numbers excluding and including zero, respectively. The set of  $n \times m$  matrices with values in  $\mathbb{F}$  ( $\mathbb{F} = \mathbb{R}$ ,  $\mathbb{R}_{>0}$ , or  $\mathbb{R}_{\geq 0}$ ) is denoted by  $\mathbf{M}_{n \times m}(\mathbb{F})$  (abbreviated as  $\mathbf{M}_n(\mathbb{F})$  whenever  $m = n$ ).  $\mathbf{GL}_n(\mathbb{F})$  and  $\mathbf{Sym}_n(\mathbb{F})$  represents the groups of invertible and symmetric matrices, respectively, with values in  $\mathbb{F}$ ; the identity ma-

trix on  $\mathbb{R}^n$  is indicated with  $I_n$ . A positive-definite matrix is noted as  $\mathbf{M}_n(\mathbb{R}) \ni Q \succ 0$ . The standard Euclidean norm on  $\mathbb{R}^n$  is indicated with  $\|\cdot\|_2$ ; matrix norms are simply denoted by  $\|\cdot\|$ .  $L^2((0, 1); \mathbb{R}^n)$  denotes the Hilbert space of square-integrable functions on  $(0, 1)$  with values in  $\mathbb{R}^n$ , endowed with inner product  $\langle \zeta_1, \zeta_2 \rangle_{L^2((0, 1); \mathbb{R}^n)} = \int_0^1 \zeta_1^T(\xi) \zeta_2(\xi) d\xi$  and induced norm  $\|\zeta(\cdot)\|_{L^2((0, 1); \mathbb{R}^n)}$ . The Hilbert space  $H^1((0, 1); \mathbb{R}^n)$  consists of functions  $\zeta \in L^2((0, 1); \mathbb{R}^n)$  whose weak derivative also belongs to  $L^2((0, 1); \mathbb{R}^n)$ ; it is naturally equipped with norm  $\|\zeta(\cdot)\|_{H^1((0, 1); \mathbb{R}^n)}^2 \triangleq \|\zeta(\cdot)\|_{L^2((0, 1); \mathbb{R}^n)}^2 + \left\| \frac{\partial \zeta(\cdot)}{\partial \xi} \right\|_{L^2((0, 1); \mathbb{R}^n)}^2$ . For a matrix-valued function  $K(\xi)$ ,  $\|K(\cdot)\|_\infty \triangleq \sup_{\xi \in [0, 1]} \|K(\xi)\|$ .  $C^k([0, T]; \mathcal{Z})$  ( $k \in \{1, 2, \dots, \infty\}$ ) denotes the space of  $k$ -times continuously differentiable functions on  $[0, T]$  with values in  $\mathcal{Z}$  (for  $T = \infty$ , the interval  $[0, T]$  is identified with  $\mathbb{R}_{\geq 0}$ ). Given two Hilbert spaces  $\mathcal{V}$  and  $\mathcal{W}$ ,  $\mathcal{L}(\mathcal{V}; \mathcal{W})$  denotes the spaces of linear operators from  $\mathcal{V}$  to  $\mathcal{W}$  (abbreviated  $\mathcal{L}(\mathcal{V})$  if  $\mathcal{V} = \mathcal{W}$ ).

## 2 Model description and preliminaries

This section is dedicated to introducing the considered family of semilinear single-track models, along with the main assumptions formulated about their dynamics. In particular, the governing equations of the model are presented in Section 2.1, whereas mild structural assumptions are postulated in Section 2.2, where some preliminary results are also collected.

### 2.1 Model description

In the following, Section 2.1.1 reviews the governing equations of the semilinear single-track models to the extent that is necessary to understand the manuscript, whereas Section 2.1.2 introduces a compact state-space representation more amenable to mathematical analysis.

#### 2.1.1 Lateral vehicle dynamics with distributed tire friction dynamics

As illustrated schematically in Figure 1, this paper examines semilinear single-track models that govern the lateral dynamics of a road vehicle traveling at a constant cruising speed, and subjected to slow-varying wind disturbances. The model presented here is adapted from Romano, Aamo, Åslund, et al. (2026b), but with some state variables restated in a nondimensional form that is more amenable to singular perturbation analysis. In particular, for sufficiently small steering inputs, the linear ODE describing the rigid vehicle dynamics may be deduced to be (Guiggiani 2023)

$$\dot{\beta}(t) = -\frac{1}{mv_x} (F_{y1}(t) + F_{y2}(t) - F_w) - r(t), \quad (1a)$$

$$\dot{r}(t) = -\frac{1}{I_z} (l_1 F_{y1}(t) - l_2 F_{y2}(t) - l_w F_w), \quad t \in (0, T), \quad (1b)$$

where the lumped states  $\beta(t)$ ,  $r(t) \in \mathbb{R}$  are the vehicle's sideslip angle and yaw rate,  $v_x \in \mathbb{R}_{>0}$  is its constant longi-

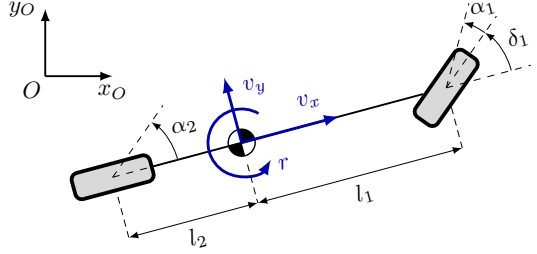


Figure 1: Single-track vehicle model.

tudinal speed,  $m \in \mathbb{R}_{>0}$  and  $I_z \in \mathbb{R}_{>0}$  denote respectively the vehicle mass and moment of inertia of the center of gravity around the vertical axis, and  $l_1, l_2 \in \mathbb{R}_{>0}$  are the front and rear axle lengths. The external force  $F_w \in \mathbb{R}$  represents a constant or slow-varying perturbation term generated by a lateral wind gust, and  $l_w \in \mathbb{R}$  denotes the offset of its point of application from the center of gravity (Guiggiani 2023). In turn, adopting a distributed friction model (Romano, Aamo, Åslund, et al. 2025; Romano, Aamo, Åslund, et al. 2026a), the tire forces  $F_{y1}(t)$ ,  $F_{y2}(t) \in \mathbb{R}$  may be calculated as

$$F_{yi}(t) = F_{zi} \int_0^1 \bar{p}_i(\xi) \left[ \bar{\sigma}_{0,i} z_i(\xi, t) + \bar{\sigma}_{1,i} \frac{dz(\xi, t)}{dt} \right] d\xi + 2F_{z,i} \bar{\sigma}_{2,i} \alpha_i(\beta(t), r(t), \delta_i(t)), \quad i \in \{1, 2\}, \quad (2)$$

where the distributed state  $z_i(\xi, t) \in \mathbb{R}$ ,  $i = \{1, 2\}$ , represents the nondimensional deflection of a bristle schematizing a tire rubber particle inside the contact patch,  $\alpha_i(\beta(t), r(t), \delta_i(t)) \in \mathbb{R}$  the corresponding apparent slip angle,  $F_{zi} \in \mathbb{R}_{>0}$  denotes the vertical force acting on the tire,  $\bar{p}_i \in C^1([0, 1]; \mathbb{R}_{\geq 0})$  is the nondimensional vertical pressure distribution, and

$$\bar{\sigma}_{0,i} \triangleq \sigma_{0,i} L_i, \quad (3a)$$

$$\bar{\sigma}_{1,i} \triangleq \sigma_{1,i} L_i, \quad (3b)$$

$$\bar{\sigma}_{2,i} \triangleq \sigma_{2,i} v_x, \quad i \in \{1, 2\}, \quad (3c)$$

being  $\sigma_{0,i} \in \mathbb{R}_{>0}$  the normalized micro-stiffness coefficient,  $\sigma_{1,i} \in \mathbb{R}_{\geq 0}$  the normalized micro-damping coefficient, and  $\sigma_{2,i} \in \mathbb{R}_{\geq 0}$  the viscous coefficient (Romano, Aamo, Åslund, et al. 2025). In turn, for a tire with a rigid carcass, the bristle dynamics obeys the following semilinear PDE (Romano, Aamo, Åslund, et al. 2026b):

$$\begin{aligned} \bar{L}_i \frac{\partial z_i(\xi, t)}{\partial t} + \frac{1}{\bar{L}_i} \frac{\partial z_i(\xi, t)}{\partial \xi} &= -\frac{1}{\bar{L}_i} \frac{\bar{\sigma}_{0,i} |\alpha_i(\beta(t), r(t), \delta_i(t))|}{\bar{g}_i(\alpha_i(\beta(t), r(t), \delta_i(t)))} \\ &\times z_i(\xi, t) + \frac{2}{\bar{L}_i} \frac{\bar{\mu}_i(\alpha_i(\beta(t), r(t), \delta_i(t)))}{\bar{g}_i(\alpha_i(\beta(t), r(t), \delta_i(t)))} \alpha_i(\beta(t), r(t), \delta_i(t)), \end{aligned} \quad (\xi, t) \in (0, 1) \times (0, T), \quad (4a)$$

$$z_i(0, t) = 0, \quad (4b)$$

with

$$\bar{L}_i \triangleq \frac{L_i}{\bar{L}}, \quad i \in \{1, 2\}, \quad (5)$$

where  $L_i \in \mathbb{R}_{>0}$  indicates the contact patch length,  $\bar{\mu}_i \in C^0(\mathbb{R}; [\mu_{\min}, \infty))$ , with  $\mu_{\min} \in \mathbb{R}_{>0}$ , the friction coefficient as a function of the slip angle, and the function  $|\cdot|_\varepsilon \in C^0(\mathbb{R}; \mathbb{R}_{\geq 0})$  denotes the (possibly regularized<sup>1</sup>) absolute value, converging uniformly to  $|\cdot|$  in  $C^0(\mathbb{R}; \mathbb{R}_{\geq 0})$  for  $\varepsilon \rightarrow 0$ . Distributed friction models accommodated by (2) and (4) include the Dahl model, as well as the LuGre and FrBD formulations with the damping term modeled as a linear function of the total time derivative of the bristle deformation<sup>2</sup>.

Alternatively, for a tire with a flexible tire carcass, and  $\bar{\sigma}_{1,i} = \bar{\sigma}_{2,i} = 0$ ,  $i \in \{1, 2\}$ , in (2) (which also implies  $\bar{g}_i(\cdot) = \bar{\mu}_i(\cdot)$ , see Romano, Aamo, Åslund, et al. (2026b)), the PDE governing the bristle dynamics may be deduced as follows:

$$\begin{aligned} \frac{\bar{L}}{v_x} \frac{\partial z_i(\xi, t)}{\partial t} + \frac{1}{\bar{L}_i} \frac{\partial z_i(\xi, t)}{\partial \xi} &= -\frac{1}{\bar{L}_i} \frac{\bar{\sigma}_{0,i} \left| \alpha_i(\beta(t), r(t), \delta_i(t)) \right|_\varepsilon}{\bar{\mu}_i(\alpha_i(\beta(t), r(t), \delta_i(t)))} \\ &\times \left( z_i(\xi, t) - \psi_i \int_0^1 \bar{p}_i(\xi) z_i(\xi) d\xi \right) \\ &+ \frac{\psi_i}{\bar{L}_i} \left( \bar{p}_i(1) z_i(1) - \int_0^1 \frac{d\bar{p}_i(\xi)}{d\xi} z_i(\xi) d\xi \right) \\ &+ 2 \frac{\phi_i}{\bar{L}_i} \alpha_i(\beta(t), r(t), \delta_i(t)), \quad (\xi, t) \in (0, 1) \times (0, T), \end{aligned} \quad (6a)$$

$$z_i(0, t) = 0, \quad (6b)$$

where the constants  $\phi_i \in (0, 1]$  and  $\psi_i \in [0, 1]$  are structural parameters connected with the flexibility of the tire carcass, identically satisfying  $\phi_i + \psi_i = 1$ ,  $i \in \{1, 2\}$ .

Finally, the parameter  $\bar{L} \in \mathbb{R}_{>0}$  appearing in both (4a) and (6a) represents a characteristic length of the problem (4). For a single-track vehicle model with rigid tire carcass, it may be defined, for instance, as  $\bar{L} \triangleq (L_1 + L_2)/2$  or  $\bar{L} \triangleq L_1 L_2 / (L_1 + L_2)$ . For a model with flexible tire carcass, alternative formulations are given by  $\bar{L} \triangleq (\lambda_1 + \lambda_2)/2$  or  $\bar{L} \triangleq \lambda_1 \lambda_2 / (\lambda_1 + \lambda_2)$ , where  $\lambda_i \in \mathbb{R}_{>0}$  denotes the relaxation length of the tire. For example, assuming a constant pressure distribution inside the contact patch gives  $\lambda_i \triangleq L_i/\phi_i$ .

The apparent slip angles in (2), (4a), and (6a) are given by

$$\alpha_1(\beta(t), r(t), \delta_1(t)) = \beta(t) + \frac{l_1}{v_x} r(t) - \delta_1(t), \quad (7a)$$

$$\alpha_2(\beta(t), r(t), \delta_2(t)) = \beta(t) - \frac{l_2}{v_x} r(t) - \chi \delta_2(t), \quad (7b)$$

being  $\delta_1(t), \delta_2(t) \in \mathbb{R}$  the steering inputs at the front and rear axles, respectively, and  $\chi \in \{0, 1\}$  a parameter describing the actuation at the rear wheels.

<sup>1</sup>It is common in engineering practice to replace the absolute value with differentiable functions  $|\cdot|_\varepsilon \in C^1(\mathbb{R}; \mathbb{R}_{\geq 0})$  (Rill, Schaeffer, and Schuderer 2024; Schuderer, Rill, and Schaeffer 2025), such as  $|v|_\varepsilon \triangleq \sqrt{v^2 + \varepsilon}$ , for some  $\varepsilon \in \mathbb{R}_{>0}$ . This paper considers  $\varepsilon \in \mathbb{R}_{\geq 0}$ .

<sup>2</sup>Model variants replacing the total time derivative with the partial one in the definition of the damping term in (2) do not fit the proposed singular perturbation framework. In this context, it is, however, worth mentioning that the partial time derivative does not represent a real deformation velocity, as opposed to the total one. Besides, there are also several mathematical arguments in favor of the adoption of the total time derivative, as extensively discussed in Romano, Aamo, Åslund, et al. (2025) and Romano, Aamo, Åslund, et al. (2026a).

Equations (1)-(7) completely determine the lateral motion of the single-track model. As explained next in Section 2.1.2, they may be restated in a compact form which is more suited to mathematical analysis.

### 2.1.2 State-space representation

Introducing the time-scale parameter  $\mathbb{R}_{>0} \ni \epsilon \triangleq \bar{L}/v_x$ , and defining  $\mathbb{R}^2 \ni X(t) \triangleq [\beta(t) \ r(t)]^T$ ,  $\mathbb{R}^2 \ni z(\xi, t) \triangleq [z_1(\xi, t) \ z_2(\xi, t)]^T$ ,  $\mathbb{R}^2 \ni U(t) \triangleq [\delta_1(t) \ \delta_2(t)]^T$ ,  $\mathbb{R}^2 \ni \alpha(X(t), U(t)) = [\alpha_1(X(t), U(t)) \ \alpha_2(X(t), U(t))]^T \triangleq [\alpha_1(\beta(t), r(t), \delta_1(t)) \ \alpha_2(\beta(t), r(t), \delta_2(t))]^T$ , and  $\mathbb{R}^2 \ni b \triangleq [\frac{F_w}{mv_x} \ \frac{l_w F_w}{I_z}]^T$ , (1)-(7) may be recast in the form<sup>3</sup>

$$\begin{aligned} \dot{X}(t) &= A_1 X(t) + G_1 \left[ (\mathcal{K}_1 z)(t) + \Sigma(\alpha(X(t), U(t))) (\mathcal{K}_2 z)(t) \right] \\ &\quad + G_1 h_1(\alpha(X(t), U(t))) + b, \quad t \in (0, T), \end{aligned} \quad (8a)$$

$$\begin{aligned} \epsilon \frac{\partial z(\xi, t)}{\partial t} + \Lambda \frac{\partial z(\xi, t)}{\partial \xi} &= \Sigma(\alpha(X(t), U(t))) \\ &\times [z(\xi, t) + (\mathcal{K}_3 z)(t)] + (\mathcal{K}_4 z)(t) \\ &+ h_2(\alpha(X(t), U(t))), \quad (\xi, t) \in (0, 1) \times (0, T), \end{aligned} \quad (8b)$$

$$z(0, t) = 0, \quad t \in (0, T), \quad (8c)$$

where the apparent slip angle vector  $\alpha \in C^1(\mathbb{R}^4; \mathbb{R}^2)$  may be expressed as

$$\alpha(X, U) \triangleq A_2 X + G_2 U. \quad (9)$$

In (8) and (9), the matrix  $\mathbf{GL}_2(\mathbb{R}) \cap \mathbf{Sym}_2(\mathbb{R}) \ni \Lambda \succ 0$  collects the transport velocities,  $\Sigma \in C^0(\mathbb{R}^2; \mathbf{M}_2(\mathbb{R}))$  represents the nonlinear source matrix,  $A_1, A_2, G_1, G_2 \in \mathbf{M}_2(\mathbb{R})$  are matrices with constant coefficients, and  $h_1, h_2 \in C^0(\mathbb{R}^2; \mathbb{R}^2)$  are vector-valued functions. Finally, the operators  $(\mathcal{K}_1 \zeta), (\mathcal{K}_2 \zeta), (\mathcal{K}_3 \zeta)$ , and  $(\mathcal{K}_4 \zeta)$  satisfy  $\mathcal{K}_1, \mathcal{K}_2, \mathcal{K}_3 \in \mathcal{L}(L^2((0, 1); \mathbb{R}^2); \mathbb{R}^2)$ , and  $\mathcal{K}_4 \in \mathcal{L}(H^1((0, 1); \mathbb{R}^2); \mathbb{R}^2)$ , with

$$(\mathcal{K}_1 \zeta) \triangleq \int_0^1 K_1(\xi) \zeta(\xi) d\xi, \quad (10a)$$

$$(\mathcal{K}_2 \zeta) \triangleq \int_0^1 K_2(\xi) \zeta(\xi) d\xi, \quad (10b)$$

$$(\mathcal{K}_3 \zeta) \triangleq \int_0^1 K_3(\xi) \zeta(\xi) d\xi, \quad (10c)$$

$$(\mathcal{K}_4 \zeta) \triangleq \int_0^1 K_4(\xi) \zeta(\xi) d\xi + K_5 \zeta(1), \quad (10d)$$

where  $K_1, K_2, K_3, K_4 \in C^0([0, 1]; \mathbf{M}_2(\mathbb{R}))$ , and  $K_5 \in \mathbf{M}_2(\mathbb{R})$ . Equations (8)-(10) accommodate semilinear single-track vehicle models with both a rigid and flexible tire carcass, as formalized below in Parametrizations 2.1 and 2.2.

<sup>3</sup>Alternatively, the term  $b$  in (8a) may also model disturbances generated by road banking, for instance by specifying  $b = [g \sin \vartheta \cos \phi \ 0]^T$ , where  $\vartheta$  denotes the bank angle, and  $\phi$  the angle between the heading of the vehicle and the tangent to the road path (Markolefas, Guiggiani, and Georgantzinos 2024).

**Parametrization 2.1** (Semilinear single-track models with a rigid tire carcass). *Semilinear single-track models with a rigid carcass admit a state-space representation in the form described by (8)-(10), with*

$$\begin{aligned}
A_1 &\triangleq \begin{bmatrix} 0 & -1 \\ 0 & 0 \end{bmatrix}, \quad G_1 \triangleq - \begin{bmatrix} \frac{1}{mv_x} & \frac{1}{mv_x} \\ \frac{l_1}{I_z} & -\frac{l_2}{I_z} \end{bmatrix}, \\
K_1(\xi) &\triangleq \begin{bmatrix} F_{z1}\bar{\sigma}_{0,1}\bar{p}_1(\xi) & 0 \\ 0 & F_{z2}\bar{\sigma}_{0,2}\bar{p}_2(\xi) \end{bmatrix}, \\
K_2(\xi) &\triangleq \begin{bmatrix} F_{z1}\bar{\sigma}_{1,1}\bar{p}_1(\xi) & 0 \\ 0 & F_{z2}\bar{\sigma}_{1,2}\bar{p}_2(\xi) \end{bmatrix}, \\
\Lambda &\triangleq \begin{bmatrix} \frac{1}{\bar{L}_1} & 0 \\ 0 & \frac{1}{\bar{L}_2} \end{bmatrix}, \quad \Sigma(\alpha) \triangleq \begin{bmatrix} -\frac{\bar{\sigma}_{0,1}|\alpha_1|_\varepsilon}{\bar{L}_1\bar{g}_1(\alpha_1)} & 0 \\ 0 & -\frac{\bar{\sigma}_{0,2}|\alpha_2|_\varepsilon}{\bar{L}_2\bar{g}_2(\alpha_2)} \end{bmatrix}, \\
h_1(\alpha) &\triangleq 2 \begin{bmatrix} F_{z1}\left(\bar{\sigma}_{1,1}\frac{\bar{\mu}_1(\alpha_1)}{\bar{L}_1\bar{g}_1(\alpha_1)} + \bar{\sigma}_{2,1}\right)\alpha_1 \\ F_{z2}\left(\bar{\sigma}_{1,2}\frac{\bar{\mu}_2(\alpha_2)}{\bar{L}_2\bar{g}_2(\alpha_2)} + \bar{\sigma}_{2,2}\right)\alpha_2 \end{bmatrix}, \\
h_2(\alpha) &\triangleq 2 \begin{bmatrix} \frac{\bar{\mu}_1(\alpha_1)}{\bar{L}_1\bar{g}_1(\alpha_1)}\alpha_1 \\ \frac{\bar{\mu}_2(\alpha_2)}{\bar{L}_2\bar{g}_2(\alpha_2)}\alpha_2 \end{bmatrix}, \tag{11}
\end{aligned}$$

$K_3 = K_4 = K_5 = 0$ , and the matrices in (9) reading

$$A_2 \triangleq \begin{bmatrix} 1 & \frac{l_1}{v_x} \\ 1 & -\frac{v_x}{l_2} \end{bmatrix}, \quad G_2 \triangleq - \begin{bmatrix} 1 & 0 \\ 0 & \chi \end{bmatrix}. \tag{12}$$

**Parametrization 2.2** (Semilinear single-track models with a flexible tire carcass). *Semilinear single-track models with a flexible tire carcass may be put compactly in the form described by (8)-(10), with  $A_1, G_1, K_1$ , and  $\Lambda$  as in (11),  $K_2 = 0$ ,  $h_1(\alpha) = 0$ ,  $A_2$  and  $G_2$  according to (12), and*

$$\begin{aligned}
K_3(\xi) &\triangleq - \begin{bmatrix} \psi_1\bar{p}_1(\xi) & 0 \\ 0 & \psi_2\bar{p}_2(\xi) \end{bmatrix}, \\
K_4(\xi) &\triangleq - \begin{bmatrix} \frac{\psi_1}{\bar{L}_1} \frac{d\bar{p}_1(\xi)}{d\xi} & 0 \\ 0 & \frac{\psi_2}{\bar{L}_2} \frac{d\bar{p}_2(\xi)}{d\xi} \end{bmatrix}, \\
K_5 &\triangleq \begin{bmatrix} \frac{\psi_1}{\bar{L}_1}\bar{p}_1(1) & 0 \\ 0 & \frac{\psi_2}{\bar{L}_2}\bar{p}_2(1) \end{bmatrix}, \\
\Sigma(\alpha) &\triangleq \begin{bmatrix} -\frac{\bar{\sigma}_{0,1}|\alpha_1|_\varepsilon}{\bar{L}_1\bar{\mu}_1(\alpha_1)} & 0 \\ 0 & -\frac{\bar{\sigma}_{0,2}|\alpha_2|_\varepsilon}{\bar{L}_2\bar{\mu}_2(\alpha_2)} \end{bmatrix}, \\
h_2(\alpha) &\triangleq 2 \begin{bmatrix} \frac{\phi_1}{\bar{L}_1} & 0 \\ 0 & \frac{\phi_2}{\bar{L}_2} \end{bmatrix} \alpha. \tag{13}
\end{aligned}$$

Equations (8)-(10) describe a semilinear hyperbolic ODE-PDE system. From a mathematical perspective, the ODE-PDE interconnection (8) is (locally) well-posed. In particular, this paper considers the Hilbert space  $\mathcal{X} \triangleq \mathbb{R}^2 \times$

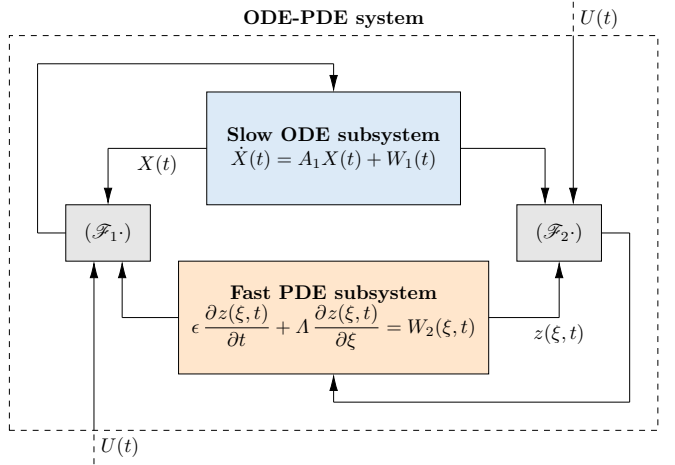


Figure 2: Schematic representation of the ODE-PDE interconnection (8).

$L^2((0, 1); \mathbb{R}^2)$ , equipped with norm  $\|(Z, \zeta(\cdot))\|_{\mathcal{X}}^2 \triangleq \|Z\|_2^2 + \|\zeta(\cdot)\|_{L^2((0, 1); \mathbb{R}^2)}^2$ . Theorem 2.1 below enounces local well-posedness results for the *mild solution* of (8).

**Theorem 2.1** (Local existence and uniqueness of mild solutions). *Suppose that  $\Sigma \in C^0(\mathbb{R}^2; \mathbf{M}_2(\mathbb{R}))$  and  $h_1, h_2 \in C^0(\mathbb{R}^2; \mathbb{R}^2)$  are locally Lipschitz continuous, and  $U \in C^0([0, T]; \mathbb{R}^2)$ . Then, for all initial conditions (ICs)  $(X_0, z_0) \triangleq (X(0), z(\cdot, 0)) \in \mathcal{X}$ , there exists  $t_{\max} \leq \infty$  such that the ODE-PDE system (8) admits a unique mild solution  $(X, z) \in C^0([0, t_{\max}); \mathcal{X})$ . Moreover, if  $t_{\max} < \infty$ ,  $\|(X(t), z(\cdot, t))\|_{\mathcal{X}} \rightarrow \infty$  for  $t \rightarrow t_{\max}$ .*

*Proof.* See Romano, Aamo, Åslund, et al. (2026b).  $\square$

A schematic of the ODE-PDE system (8) is illustrated in Figure 2, where, for convenience of notation,  $\mathbb{R}^2 \ni W_1(t) \triangleq (\mathcal{F}_1(X, U, z))(t)$  and  $\mathbb{R}^2 \ni W_2(\xi, t) \triangleq (\mathcal{F}_2(X, U, z))(\xi, t)$ , with  $(\mathcal{F}_1(X, U, z))(t) \triangleq G_1(\mathcal{K}_1 z)(t) + G_1 \Sigma(\alpha(X(t), U(t))) (\mathcal{K}_2 z)(t) + G_1 h_1(\alpha(X(t), U(t))) + b$  and  $(\mathcal{F}_2(X, U, z))(\xi, t) \triangleq \Sigma(\alpha(X(t), U(t))) [z(\xi, t) + (\mathcal{K}_3 z)(t)] + (\mathcal{K}_4 z)(t) + h_2(\alpha(X(t), U(t)))$ .

The objective of this paper consists of studying the (local) stability and stabilization of the hyperbolic ODE-PDE system (8), exploiting the time-scale separation between the slow ODE and fast PDE subsystems (8a) and (8b), respectively. Indeed, at sufficiently high longitudinal speeds  $v_x$ , the tire dynamics evolve much faster than the rigid body ones. This informal argument has traditionally motivated studying the stability of road vehicles using reduced-order descriptions that approximate the transient tire forces with their steady-state solutions. In a similar context, controllers and state observers are typically designed by neglecting tire dynamics.

In the output-feedback stabilization case, only the yaw rate  $r(t)$  is supposed to be available for measurement, which is the standard assumption in the literature. Accordingly, the measurement output  $Y(t) \in \mathbb{R}$  may be specified in the form

$$Y(t) = CX(t), \tag{14}$$

with  $C \in \mathbf{M}_{1 \times 2}(\mathbb{R})$  reading

$$C \triangleq \begin{bmatrix} 0 & 1 \end{bmatrix}. \quad (15)$$

## 2.2 Assumptions and preliminaries

This Section introduces the main assumptions required to synthesize the proposed controllers and observer.

### 2.2.1 Structural assumptions

The structural assumptions formulated in this paper concern the fast PDE subsystem (8b), and reflect the fact that rolling friction is a dissipative phenomenon.

**Assumption 2.1** (Strict dissipativity). *There exists  $C^0([0, 1]; \mathbf{Sym}_2(\mathbb{R})) \ni \mathcal{Q} \triangleq \text{diag}\{\mathcal{Q}_1, \mathcal{Q}_2\}$ , with  $\mathcal{Q}(\xi) \succ 0$ , such that, for all  $y \in \mathbb{R}^2$ , the unbounded operator  $(\mathcal{A}, \mathcal{D}(\mathcal{A}))$ , defined by*

$$(\mathcal{A}\zeta)(\xi) \triangleq -\Lambda \frac{\partial \zeta(\xi)}{\partial \xi} + (\mathcal{K}_3\zeta)(\xi), \quad (16a)$$

$$\mathcal{D}(\mathcal{A}) \triangleq \left\{ \zeta \in H^1((0, 1); \mathbb{R}^2) \mid \zeta(0) = 0 \right\}, \quad (16b)$$

satisfies

$$\text{Re}\langle \mathcal{A}\zeta, \mathcal{Q}\zeta \rangle_{L^2((0,1); \mathbb{R}^2)} \leq -\omega \|\zeta(\cdot)\|_{L^2((0,1); \mathbb{R}^2)}^2, \quad (17)$$

for all  $\zeta \in \mathcal{D}(\mathcal{A})$  and some  $\omega \in \mathbb{R}_{>0}$ .

Assumption 2.1 implies that  $(\mathcal{A}, \mathcal{D}(\mathcal{A}))$  generates an exponentially stable  $C_0$ -semigroup on  $L^2((0, 1); \mathbb{R}^2)$ . Its physical interpretation is that rolling contact processes, when considered in isolation, are stable (in fact, they are even dissipative).

**Assumption 2.2** (Dissipativity and Lipschitz continuity). *For every  $(y, \zeta) \in \mathbb{R}^2 \times L^2((0, 1); \mathbb{R}^2)$ , the matrix  $\Sigma(y) \in \mathbf{M}_2(\mathbb{R})$  satisfies*

$$\int_0^1 \zeta^T(\xi) \mathcal{Q}(\xi) \Sigma(y) [\zeta(\xi) + (\mathcal{K}_2\zeta)] d\xi \leq 0. \quad (18)$$

Additionally, it is globally Lipschitz continuous, that is, there exists  $L_\Sigma \in \mathbb{R}_{\geq 0}$  such that

$$\|\Sigma(y_1) - \Sigma(y_2)\| \leq L_\Sigma \|y_1 - y_2\|_2, \quad (19)$$

for all  $y_1, y_2 \in \mathbb{R}^2$ .

Some comments are in order. First, the dissipativity inequalities (17) and (18) in Assumptions 2.1 and 2.2 are trivial to prove for  $\psi_i = 0$ ,  $i \in \{1, 2\}$ . More generally, the bounds (17) and (18) may be verified for several combinations of model parameters, for instance by resorting to passivity arguments, and choosing the matrix  $\mathcal{Q}(\xi)$  as a multiple of  $K_1(\xi)$  (the reader may consult Romano, Aamo, Krstić, et al. (2025) for further details on this matter). Finally, the Lipschitz condition (19) holds for the Dahl, LuGre, and FrBD models, as well as all the formulations considered in Romano, Aamo, Åslund, et al. (2026b). In fact, in some cases, the matrix-valued function  $\Sigma \in C^1(\mathbb{R}^2; \mathbf{M}_2(\mathbb{R}))$  is uniformly bounded, which may ensure global well-posedness for the mild solutions of the open-loop ODE-PDE system (8)

(see Romano, Aamo, Åslund, et al. (2026b)). Together, Assumptions 2.1 and 2.2 permit recovering some preliminary results, as formalized next in Proposition 2.1 and Lemma 2.1.

**Proposition 2.1** (Strict dissipativity). *Suppose that Assumptions 2.1 and 2.2 hold. Then, for all  $y \in \mathbb{R}^2$ , the unbounded operator  $(\mathcal{A}_\Sigma(y), \mathcal{D}(\mathcal{A}_\Sigma(y)))$ , defined by*

$$(\mathcal{A}_\Sigma(y)\zeta)(\xi) \triangleq \Sigma(y)[\zeta(\xi) + (\mathcal{K}_2\zeta)] + (\mathcal{A}\zeta)(\xi), \quad (20a)$$

$$\mathcal{D}(\mathcal{A}_\Sigma(y)) = \mathcal{D}(\mathcal{A}) \triangleq \left\{ \zeta \in H^1((0, 1); \mathbb{R}^2) \mid \zeta(0) = 0 \right\}, \quad (20b)$$

also generates an exponentially stable  $C_0$ -semigroup on  $L^2((0, 1); \mathbb{R}^2)$ . In particular,

$$\text{Re}\langle \mathcal{A}_\Sigma(y)\zeta, \mathcal{Q}\zeta \rangle_{L^2((0,1); \mathbb{R}^2)} \leq -\omega \|\zeta(\cdot)\|_{L^2((0,1); \mathbb{R}^2)}^2, \quad (21)$$

for all  $(y, \zeta) \in \mathbb{R}^2 \times \mathcal{D}(\mathcal{A}_\Sigma(y))$ , with the same  $\omega \in \mathbb{R}_{>0}$  as in (17).

*Proof.* The assertion is an immediate consequence of the inequalities (17) and (18).  $\square$

**Lemma 2.1.** *Suppose that Assumptions 2.1 and 2.2 hold. Then, for every  $\mathbb{R}^2 \ni y = [y_1 \ y_2]^T$ , the nonlocal ODE*

$$\Lambda \frac{\partial \varphi(\xi, y)}{\partial \xi} = \Sigma(y)[\varphi(\xi, y) + (\mathcal{K}_3\varphi)(y)] + (\mathcal{K}_4\varphi)(y) + h_2(y), \quad \xi \in (0, 1) \quad (22a)$$

$$\varphi(0, y) = 0, \quad (22b)$$

admits a unique solution  $\varphi(\cdot, y) \in C^1([0, 1]; \mathbb{R}^2)$ , with  $\mathbb{R}^2 \ni \varphi(\xi, y) = [\varphi_1(\xi, y_1) \ \varphi_2(\xi, y_2)]^T$ .

*Proof.* The result is a consequence of inequality (21).  $\square$

For what follows, it is also beneficial to define the function  $\mathbb{R}^2 \ni \Phi(\cdot) \triangleq [\Phi_1(\cdot) \ \Phi_2(\cdot)]^T$  as

$$\Phi(y) \triangleq (\mathcal{K}_1\varphi)(y) + \Sigma(y)(\mathcal{K}_2\varphi)(y) + h_1(y). \quad (23)$$

Utilizing (22) and (23), the equilibria  $(X^*, z^*) \in \mathbb{R}^2 \times \mathcal{D}(\mathcal{A})$  of (8) associated with a constant input  $U^* \in \mathbb{R}^2$  are given by

$$A_1 X^* + G_1 F_y^* + b = 0, \quad (24a)$$

$$F_y^* - \Phi(\alpha^*) = 0, \quad (24b)$$

$$z^*(\xi) - \varphi(\xi, \alpha^*) = 0, \quad (24c)$$

$$\alpha^* - A_2 X^* - G_2 U^* = 0, \quad (24d)$$

where  $\mathbb{R}^2 \ni F_y^* = [F_{y1}^* \ F_{y2}^*]^T$  and  $\mathbb{R}^2 \ni \alpha^* = [\alpha_1^* \ \alpha_2^*]^T$  denote respectively the steady-state tire forces and apparent slip angles.

In particular, the following Assumption 2.3 is postulated concerning the functions  $\varphi(\xi, \cdot)$  and  $\Phi(\cdot)$ .

**Assumption 2.3.** *The functions  $\varphi(\xi, \cdot) \in C^1([0, 1] \times \mathbb{R}^2; \mathbb{R}^2)$ ,  $\Phi \in C^1(\mathbb{R}^2; \mathbb{R}^2)$ . Moreover, there exists  $M_\varphi \in \mathbb{R}_{\geq 0}$  such that*

$$\max_{y \in \mathbb{R}^2} \left\| \frac{\partial \varphi(\cdot, y)}{\partial y} \right\|_\infty \leq M_\varphi. \quad (25)$$

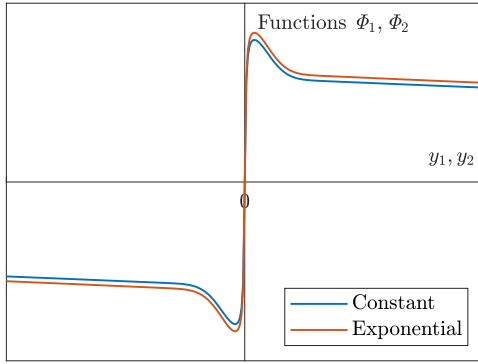


Figure 3: Typical trends of the function  $\Phi(\cdot)$  obtained for constant and exponentially decreasing pressure distributions  $\bar{p}_i(\xi)$ ,  $i \in \{1, 2\}$ .

Assumption 2.3 is always verified in practice. For instance, Figure 3 illustrates some typical trends for the function  $\Phi(\cdot)$ , obtained for constant and exponentially decreasing pressure distributions  $\bar{p}_i(\xi)$ ,  $i \in \{1, 2\}$ .

Before moving to the next Section 2.2.2, it is useful to introduce the matrix  $\tilde{C}(\alpha^*) \in \mathbf{M}_2(\mathbb{R})$  of generalized cornering stiffnesses as

$$\begin{aligned} \tilde{C}(\alpha^*) &= \begin{bmatrix} \tilde{C}_1(\alpha_1^*) & 0 \\ 0 & \tilde{C}_2(\alpha_2^*) \end{bmatrix} \\ &\triangleq \begin{bmatrix} \frac{d\Phi_1(y_1)}{dy_1} \Big|_{y_1=\alpha_1^*} & 0 \\ 0 & \frac{d\Phi_2(y_2)}{dy_2} \Big|_{y_2=\alpha_2^*} \end{bmatrix} = \frac{d\Phi(y)}{dy} \Big|_{y=\alpha^*}. \end{aligned} \quad (26)$$

In the vehicle dynamics literature, the quantities  $\tilde{C}_1(\alpha_1^*), \tilde{C}_2(\alpha_2^*) \in \mathbb{R}$  appearing in (26) are typically referred to as *generalized cornering stiffnesses* of the front and rear axle, respectively.

## 2.2.2 Assumptions for controller and observer design

A last set of assumptions is introduced to facilitate the design of state and output-feedback controllers. Specifically, the present work focuses on local stability and stabilization. In this context, it is necessary to define the matrices  $\tilde{A}_1(\alpha^*), \tilde{G}_1(\alpha^*) \in \mathbf{M}_2(\mathbb{R})$ :

$$\begin{aligned} \tilde{A}_1(\alpha^*) &\triangleq A_1 + G_1 \tilde{C}(\alpha^*) A_2 \\ &= - \begin{bmatrix} \frac{\tilde{C}_1(\alpha_1^*) + \tilde{C}_2(\alpha_2^*)}{mv_x} & \frac{l_1 \tilde{C}_1(\alpha_1^*) - l_2 \tilde{C}_2(\alpha_2^*)}{I_z v_x} + 1 \\ \frac{l_1 \tilde{C}_1(\alpha_1^*) - l_2 \tilde{C}_2(\alpha_2^*)}{I_z} & \frac{l_1^2 \tilde{C}_1(\alpha_1^*) + l_2^2 \tilde{C}_2(\alpha_2^*)}{I_z v_x} \end{bmatrix}, \end{aligned} \quad (27a)$$

$$\tilde{G}_1(\alpha^*) \triangleq G_1 \tilde{C}(\alpha^*) G_2 = \begin{bmatrix} \frac{\tilde{C}_1(\alpha_1^*)}{mv_x} & \chi \frac{\tilde{C}_2(\alpha_2^*)}{mv_x} \\ \frac{l_1 \tilde{C}_1(\alpha_1^*)}{I_z} & -\chi \frac{l_2 \tilde{C}_2(\alpha_2^*)}{I_z} \end{bmatrix}. \quad (27b)$$

Accordingly, stabilizability and detectability assumptions are formulated below.

**Assumption 2.4** (Stabilizability). *The pair  $(\tilde{A}_1(\alpha^*), \tilde{G}_1(\alpha^*))$  is stabilizable.*

**Assumption 2.5** (Detectability). *The pair  $(\tilde{A}_1(\alpha^*), C)$  is detectable.*

Some important considerations about the validity of Assumption 2.4 and 2.5 are formalized below in Remark 1.

**Remark 1.** *Typically,  $\tilde{C}_1(\alpha_1^*) > 0$  suffices to guarantee the controllability of the pair  $(\tilde{A}_1(\alpha^*), \tilde{G}_1(\alpha^*))$  in Assumption 2.4. Additionally, the condition  $\tilde{C}_1(\alpha_1^*)l_1 \neq \tilde{C}_2(\alpha_2^*)l_2$  ensures the observability of the pair  $(\tilde{A}_1(\alpha^*), C)$  in Assumption 2.5. Moreover, for  $\tilde{C}_1(\alpha_1^*)l_1 = \tilde{C}_2(\alpha_2^*)l_2 > 0$ ,  $\tilde{A}_1(\alpha^*)$  in (27a) is Hurwitz, which is enough to yield detectability. In practice, excluding maneuvers at the limit of handling where  $\tilde{C}_1(\alpha_1^*) = \tilde{C}_2(\alpha_2^*) = 0$ , Assumptions 2.4 and 2.5 are always fulfilled in normal operating conditions of the vehicle.*

## 3 Stability

The present Section investigates the stability of the ODE-PDE system (8). Specifically, Section 3.1 adopts a singular perturbation approach, considering the reduced and boundary layer subsystems in isolation, whereas Section 3.2 recovers a Tikhonov-like stability result for sufficiently small values of the parameter  $\epsilon$ .

### 3.1 Analysis via singular perturbation theory

By exploiting the timescale separation between the ODE and PDE equations, the stability of the interconnection (8) may be studied by considering the corresponding reduced ODE and boundary layer PDE subsystems, as separately done in Sections 3.1.1 and 3.1.2, respectively.

#### 3.1.1 Reduced ODE subsystem

In proceeding with a singular perturbation analysis, the first step consists of deriving the reduced ODE subsystem. To this end, by setting  $\epsilon = 0$  in (8b), the following nonlocal ODE is deduced for fixed  $t$ :

$$\begin{aligned} \Lambda \frac{\partial z(\xi, t)}{\partial \xi} &= \Sigma(\alpha(X(t), U(t))) [z(\xi, t) + (\mathcal{K}_3 z)(t)] \\ &\quad + (\mathcal{K}_4 z)(t) + h_2(\alpha(X(t), U(t))), \end{aligned} \quad (28a)$$

$$z(0, t) = 0, \quad t \in (0, T). \quad (28b)$$

By Lemma 2.1, for every  $t \in (0, T)$ , (28) admits a unique solution  $z(\cdot, t) \in C^1([0, 1]; \mathbb{R}^2)$  satisfying the BC (28b) in the form

$$z(\xi, t) = \varphi\left(\xi, \alpha(X(t), U(t))\right), \quad \xi \in [0, 1]. \quad (29)$$

Substituting (29) into (8a) yields

$$\dot{\bar{X}}(t) = A_1 \bar{X}(t) + G_1 \Phi\left(\alpha(\bar{X}(t), \bar{U}(t))\right) + b, \quad t \in (0, T), \quad (30)$$

where the bar notation has been introduced to indicate the ODE variables obtained for  $\epsilon = 0$ .

An equilibrium  $(X^*, U^*) \in \mathbb{R}^4$  as in (24) is now considered, along with the variables  $\mathbb{R}^2 \ni \bar{X}_\delta(t) \triangleq \bar{X}(t) - X^*$  and  $\mathbb{R}^2 \ni \bar{U}_\delta(t) \triangleq \bar{U}(t) - U^*$ . Consequently, performing an exact first-order Taylor's expansion under Assumption 2.3, and specifying  $\bar{U}_\delta(t) = 0$  provides

$$\dot{\bar{X}}_\delta(t) = \tilde{A}_1(\alpha^*) \bar{X}_\delta(t) + R(\bar{X}_\delta(t), \alpha^*), \quad t \in (0, T), \quad (31)$$

where, for every  $\alpha^* \in \mathbb{R}^2$ ,  $R(\cdot, \alpha^*) \in C^0(\mathbb{R}^2; \mathbb{R}^2)$  satisfies

$$\lim_{\|Z\|_2 \rightarrow 0} \frac{\|R(Z, \alpha^*)\|_2}{\|Z\|_2} = 0. \quad (32)$$

Local exponential stability results for the reduced ODE subsystem (31), which is equivalent to (30), are enounced by Proposition 3.1 below.

**Proposition 3.1.** *Under Assumption 2.3, consider the reduced ODE subsystem (31) along with the equilibrium  $(X^*, U^*)$ , and suppose that the matrix  $\tilde{A}_1(\alpha^*) \in \mathbf{M}_2(\mathbb{R})$  in (27a) is Hurwitz. Then, there exists  $r \in \mathbb{R}_{>0}$  such that, for all ICs  $\bar{X}_0 \triangleq \bar{X}(0) \in \mathbb{R}^2$  with  $\|\bar{X}_0 - X^*\|_2 < r$ , the unique solution  $\bar{X} \in C^0(\mathbb{R}_{\geq 0}; \mathbb{R}^2)$  to (30) satisfies*

$$\|\bar{X}(t) - X^*\|_2 \leq \beta_1(\alpha^*) e^{-\sigma_1(\alpha^*)t} \|\bar{X}_0 - X^*\|_2, \quad t \in [0, T], \quad (33)$$

for some  $\beta_1(\alpha^*), \sigma_1(\alpha^*) \in \mathbb{R}_{>0}$ .

Based on the assertion of Proposition 3.1, some interesting considerations are collected below.

**Remark 2.** *The condition on  $\tilde{A}_1(\alpha^*)$  being Hurwitz is equivalent to  $\tilde{C}_1(\alpha_1^*)l_1 < \tilde{C}_2(\alpha_2^*)l_2$ , which is the famous understeer inequality encountered in the vehicle dynamics literature.*

**Remark 3.** *The reduced ODE subsystem, in both its original and linearized variants (30) and (31), respectively, coincides with the formulations typically encountered in the literature, and obtained by disregarding the fast dynamics of the tires.*

### 3.1.2 Boundary layer PDE subsystem

The second step requires deriving the boundary layer PDE subsystem. In particular, performing the transformation

$\mathbb{R}^2 \ni \zeta(\xi, t) \triangleq z(\xi, t) - \varphi(\xi, \alpha(X(t), U(t)))$ , and introducing the time-like variable  $\mathbb{R}_{\geq 0} \ni s \triangleq t/\epsilon$  gives

$$\begin{aligned} \frac{\partial \zeta(\xi, s)}{\partial s} + \Lambda \frac{\partial \zeta(\xi, s)}{\partial \xi} &= \Sigma(\alpha(X(t), U(t))) \\ &\times [\zeta(\xi, s) + (\mathcal{K}_3 \zeta)(s)] + (\mathcal{K}_4 \zeta)(s) \\ &- \epsilon \frac{\partial \varphi(\xi, \alpha(X(t), U(t)))}{\partial t}, \quad (\xi, s) \in (0, 1) \times (0, S), \end{aligned} \quad (34a)$$

$$\zeta(0, s) = 0, \quad s \in (0, S), \quad (34b)$$

where the identity

$$\begin{aligned} \Lambda \frac{\partial \varphi(\xi, \alpha(X(t), U(t)))}{\partial \xi} &= \Sigma(\alpha(X(t), U(t))) \\ &\times [\varphi(\xi, \alpha(X(t), U(t))) + (\mathcal{K}_3 \varphi)(\alpha(X(t), U(t))) \\ &+ (\mathcal{K}_4 \varphi)(\alpha(X(t), U(t))) \\ &+ h_2(\alpha(X(t), U(t)))], \quad \xi \in [0, 1] \end{aligned} \quad (35)$$

has been used. Therefore, by setting  $\epsilon = 0$  in (34), the dynamics of the boundary layer PDE subsystem may be deduced to obey

$$\begin{aligned} \frac{\partial \bar{\zeta}(\xi, s)}{\partial s} + \Lambda \frac{\partial \bar{\zeta}(\xi, s)}{\partial \xi} &= \Sigma(\alpha(X(t), U(t))) \\ &\times [\bar{\zeta}(\xi, s) + (\mathcal{K}_3 \bar{\zeta})(s)] + (\mathcal{K}_4 \bar{\zeta})(s), \quad (36a) \\ &(\xi, s) \in (0, 1) \times (0, S), \\ \bar{\zeta}(0, s) = 0, \quad s \in (0, S), \quad (36b) \end{aligned}$$

where the bar notation has again been adopted to indicate the PDE variables corresponding to  $\epsilon = 0$ . Before enouncing the stability results for (36), it is worth clarifying that, in (36), the variable  $t$  may be regarded as a parameter, and consequently  $X(t)$  and  $U(t)$  as frozen at a certain time.

**Lemma 3.1.** *Suppose that Assumptions 2.1 and 2.2 hold. Then, for all ICs  $\bar{\zeta}_0 \triangleq \bar{\zeta}(\cdot, 0) \in L^2((0, 1); \mathbb{R}^2)$  and  $(X(t), U(t)) \in \mathbb{R}^4$ , the boundary layer PDE subsystem (36) admits a unique mild solution  $\bar{\zeta} \in C^0(\mathbb{R}_{\geq 0}; L^2((0, 1); \mathbb{R}^2))$  satisfying*

$$\|\bar{\zeta}(\cdot, s)\|_{L^2((0, 1); \mathbb{R}^2)} \leq \beta_2 e^{-\omega s} \|\bar{\zeta}_0(\cdot)\|_{L^2((0, 1); \mathbb{R}^2)}, \quad s \in [0, S], \quad (37)$$

for some  $\beta_2 \in \mathbb{R}_{>0}$ .

*Proof.* For all  $\bar{\zeta}_0 \in L^2((0, 1); \mathbb{R}^2)$  and  $(X(t), U(t)) \in \mathbb{R}^4$ , the existence and uniqueness of mild solutions  $\bar{\zeta} \in C^0(\mathbb{R}_{\geq 0}; L^2((0, 1); \mathbb{R}^2))$  follow by standard semigroup arguments. The bound (37) is immediately implied by Assumptions 2.1 and 2.2.  $\square$

The assertions of Proposition 3.1 and Lemma 3.1 are formally valid only for  $\epsilon = 0$ . The next Section 3.2 generalizes the singular perturbation analysis by considering sufficiently small values of  $\epsilon$ .

### 3.2 Stability analysis for sufficiently small $\epsilon$

Based on the preliminary results of Section 3.1, the local stability of the system (8) is studied for sufficiently small  $\epsilon$ . To this end, the ODE-PDE interconnection (8) may be recast as

$$\begin{aligned}\dot{X}_\delta(t) &= \tilde{A}_1(\alpha^*)X_\delta(t) + R(X_\delta(t), \alpha^*) + G_1(\mathcal{H}_1\zeta)(t) \\ &+ G_1\Sigma(\alpha(X(t), U^*))(\mathcal{H}_2\zeta)(t), \quad t \in (0, T),\end{aligned}$$

$$\frac{\partial \zeta(\xi, t)}{\partial t} + \frac{\Lambda}{\epsilon} \frac{\partial \zeta(\xi, t)}{\partial \xi} = \frac{1}{\epsilon} \Sigma(\alpha(X(t), U^*)) \quad (38a)$$

$$\begin{aligned}&\times [\zeta(\xi, t) + (\mathcal{H}_3\zeta)(t)] + \frac{1}{\epsilon} (\mathcal{H}_4\zeta)(t) \\ &- \frac{\partial \varphi(\xi, \alpha(X(t), U^*))}{\partial \alpha} A_2 \\ &\times [\tilde{A}_1(\alpha^*)X_\delta(t) + R(X_\delta(t), \alpha^*)] \\ &- \frac{\partial \varphi(\xi, \alpha(X(t), U^*))}{\partial \alpha} A_2 G_1 \\ &\times [(\mathcal{H}_1\zeta)(t) + \Sigma(\alpha(X(t), U^*))(\mathcal{H}_2\zeta)(t)],\end{aligned} \quad (38b)$$

$$\zeta(\xi, t) \in (0, 1) \times (0, T), \quad (38c)$$

$$\zeta(0, t) = 0, \quad t \in (0, T),$$

The following Lyapunov function candidate is considered:

$$V_1(X_\delta(t)) \triangleq \frac{1}{2} X_\delta^T(t) Q(\alpha^*) X_\delta(t), \quad (39)$$

where  $\mathbf{Sym}_2(\mathbb{R}) \ni Q(\alpha^*) \succ 0$  is chosen such that  $\tilde{A}_1(\alpha^*)Q(\alpha^*) + Q(\alpha^*)\tilde{A}_1(\alpha^*) = -2q$  for some  $q \in \mathbb{R}_{>0}$ . Differentiating (39) along the dynamics (38a) yields

$$\begin{aligned}\dot{V}_1(t) &\leq -q\|X_\delta(t)\|_2^2 + X_\delta^T(t)Q(\alpha^*)G_1 \\ &\times [(\mathcal{H}_1\zeta)(t) + \Sigma(\alpha(X(t), U^*))(\mathcal{H}_2\zeta)(t)] \\ &+ \|X_\delta(t)\|_2\|Q(\alpha^*)\|\|R(X_\delta(t), \alpha^*)\|_2, \quad t \in (0, T).\end{aligned} \quad (40)$$

By Assumption 2.2, there exists  $b_\Sigma(\alpha^*) \in \mathbb{R}_{\geq 0}$  such that

$$\|\Sigma(\alpha(X(t), U^*))\| \leq L_\Sigma\|A_2\|\|X_\delta(t)\|_2 + b_\Sigma(\alpha^*), \quad (41)$$

which gives

$$\begin{aligned}\dot{V}_1(t) &\leq -q\|X_\delta(t)\|_2^2 + \eta_1(\alpha^*)\|X_\delta(t)\|_2\|\zeta(\cdot, t)\|_{L^2((0,1);\mathbb{R}^2)} \\ &+ \eta_2\|X_\delta(t)\|_2 \left( \|X_\delta(t)\|_2\|\zeta(\cdot, t)\|_{L^2((0,1);\mathbb{R}^2)} \right. \\ &\left. + \|R(X_\delta(t), \alpha^*)\|_2 \right), \quad t \in (0, T).\end{aligned} \quad (42)$$

with

$$\eta_1(\alpha^*) \triangleq \|Q(\alpha^*)G_1\| \max \left\{ \|K_1(\cdot)\|_\infty, b_\Sigma(\alpha^*)\|K_2(\cdot)\|_\infty \right\}, \quad (43a)$$

$$\eta_2 \triangleq \max \left\{ \|Q(\alpha^*)G_1\| L_\Sigma\|A_2\|\|K_2(\cdot)\|_\infty, \|Q(\alpha^*)\| \right\}. \quad (43b)$$

A second Lyapunov function candidate is then defined as

$$V_2(\zeta(\cdot, t)) \triangleq \int_0^1 \zeta^T(\xi, t) \mathcal{Q}(\xi) \zeta(\xi, t) d\xi. \quad (44)$$

Differentiating (44) along the dynamics (38b) and imposing the BC (38c) yields

$$\begin{aligned}\dot{V}_2(t) &\leq -\frac{\omega}{\epsilon} \|\zeta(\cdot, t)\|_{L^2((0,1);\mathbb{R}^2)}^2 + \eta_3 \|\zeta(\cdot, t)\|_{L^2((0,1);\mathbb{R}^2)} \\ &\times \left( \|\tilde{A}_1(\alpha^*)\| \|X_\delta(t)\|_2 + \|R(X_\delta(t), \alpha^*)\|_2 \right. \\ &+ \|G_1\| \|K_2(\cdot)\|_\infty \|\Sigma(\alpha(X(t), U^*))\| \|\zeta(\cdot, t)\|_{L^2((0,1);\mathbb{R}^2)} \\ &\left. + \|G_1 K_1(\cdot)\|_\infty \|\zeta(\cdot, t)\|_{L^2((0,1);\mathbb{R}^2)} \right), \quad t \in (0, T),\end{aligned} \quad (45)$$

with

$$\eta_3 \triangleq M_\varphi \|\mathcal{Q}(\cdot)\|_\infty \|A_2\|. \quad (46)$$

Utilizing again (41) provides

$$\begin{aligned}\dot{V}_2(t) &\leq -\frac{\omega}{\epsilon} \left( 1 - \epsilon \frac{\eta_4(\alpha^*)}{\omega} \right) \|\zeta(\cdot, t)\|_{L^2((0,1);\mathbb{R}^2)}^2 \\ &+ \eta_5 \|X_\delta(t)\|_2 \|\zeta(\cdot, t)\|_{L^2((0,1);\mathbb{R}^2)} \\ &+ \eta_6 \|\zeta(\cdot, t)\|_{L^2((0,1);\mathbb{R}^2)} \left( \|R(X_\delta(t), \alpha^*)\|_2 \right. \\ &\left. + \|X_\delta(t)\|_2 \|\zeta(\cdot, t)\|_{L^2((0,1);\mathbb{R}^2)} \right), \quad t \in (0, T).\end{aligned} \quad (47)$$

with

$$\eta_4(\alpha^*) \triangleq \eta_3 \max \left\{ \|G_1 K_1(\cdot)\|_\infty, \|G_1\| \|K_2(\cdot)\|_\infty b_\Sigma(\alpha^*) \right\}, \quad (48a)$$

$$\eta_5(\alpha^*) \triangleq \eta_3 \|\tilde{A}_1(\alpha^*)\|, \quad (48b)$$

$$\eta_6 \triangleq \eta_3 \max \left\{ 1, L_\Sigma \|G_1\| \|K_2(\cdot)\|_\infty \|A_2\| \right\}. \quad (48c)$$

The final Lyapunov function is consequently assembled as

$$V(X_\delta(t), \zeta(\cdot, t)) \triangleq V_1(X_\delta(t)) + V_2(\zeta(\cdot, t)). \quad (49)$$

Accordingly, a straightforward application of Cauchy-Schwarz and the generalized Young's inequality for products provides

$$\begin{aligned}\dot{V}(t) &\leq -\frac{q}{2} \|X_\delta(t)\|_2^2 \\ &- \frac{\omega}{\epsilon} \left( 1 - \epsilon \frac{\eta_7(\alpha^*)}{\omega} \right) \|\zeta(\cdot, t)\|_{L^2((0,1);\mathbb{R}^2)}^2 \\ &+ \eta_8 \left( \|X_\delta(t)\|_2 + \|\zeta(\cdot, t)\|_{L^2((0,1);\mathbb{R}^2)} \right) \\ &\times \left( \|R(X_\delta(t), \alpha^*)\|_2 \right. \\ &\left. + \|X_\delta(t)\|_2 \|\zeta(\cdot, t)\|_{L^2((0,1);\mathbb{R}^2)} \right), \quad t \in (0, T),\end{aligned} \quad (50)$$

where

$$\eta_7(\alpha^*) \triangleq \eta_4(\alpha^*) + \frac{\max\{\eta_1(\alpha^*), \eta_5(\alpha^*)\}^2}{2q}, \quad (51a)$$

$$\eta_8 \triangleq \max\{\eta_2, \eta_6\}. \quad (51b)$$

Therefore, it may be inferred that there exists  $\epsilon^*(\alpha^*) \in \mathbb{R}_{>0}$  such that, for every  $\epsilon \in (0, \epsilon^*(\alpha^*))$ ,

$$\begin{aligned} \dot{V}(t) &\leq -\gamma_0(\alpha^*)V(t) \\ &+ \eta_9(\alpha^*)V^{\frac{1}{2}}(t)\left(V(t) + \left\|R(X_\delta(t), \alpha^*)\right\|_2\right), \quad (52) \\ &t \in (0, T), \end{aligned}$$

for some  $\gamma_0(\alpha^*), \eta_9(\alpha^*) \in \mathbb{R}_{>0}$ . Moreover, (32) implies that, for every  $\gamma_1 \in \mathbb{R}_{>0}$ , there exists  $r_\epsilon^*(\alpha)$  such that  $\|R(X_\delta(t), \alpha^*)\|_2 \leq \gamma_1 V^{\frac{1}{2}}(t)$  for all  $V(t) < r_\epsilon^*(\alpha^*)$ . Consider now  $r_\epsilon \in (0, r_\epsilon^*(\alpha^*))$ . For  $V(t) < r_\epsilon$ ,

$$\dot{V}(t) \leq -\gamma_0(\alpha^*)V(t) + \eta_9(\alpha^*)(\sqrt{r_\epsilon} + \gamma_1)V(t), \quad t \in (0, T). \quad (53)$$

Hence, choosing  $r_\epsilon$  such that  $\eta_9(\alpha^*)(\sqrt{r_\epsilon} + \gamma_1) < \gamma_0(\alpha^*)$  guarantees the existence of  $\gamma(\alpha^*) \in \mathbb{R}_{>0}$  such that

$$\dot{V}(t) \leq -\gamma(\alpha^*)V(t), \quad t \in (0, T), \quad (54)$$

for all  $V(t) < r_\epsilon$ . The next Theorem 3.1 asserts the main result of the paper.

**Theorem 3.1.** *Under Assumptions 2.1-2.3, consider the ODE-PDE interconnection (8) along with the equilibrium  $(X^*, U^*)$ , and the input  $U(t) = U^*$ , and suppose that the matrix  $\tilde{A}_1(\alpha^*) \in \mathbf{M}_2(\mathbb{R})$  in (27a) is Hurwitz. Then, there exist  $\epsilon^*(\alpha^*), r_\epsilon \in \mathbb{R}_{>0}$  such that, for all  $\epsilon \in (0, \epsilon^*(\alpha^*))$  and ICs  $(X_0, z_0(\cdot)) \in \mathcal{X}$  verifying  $V(0) < r_\epsilon$ , with  $V(X_\delta(t), \zeta(\cdot, t))$  as in (49), the ODE-PDE system (8) admits a unique mild solution  $(X, z) \in C^0(\mathbb{R}_{\geq 0}; \mathcal{X})$  satisfying*

$$\begin{aligned} &\|(X(t) - X^*, \zeta(\cdot, t))\|_{\mathcal{X}} \\ &\leq \beta(\alpha^*)e^{-\sigma(\alpha^*)t}\|(X_0 - X^*, \zeta_0(\cdot))\|_{\mathcal{X}}, \quad t \in [0, T], \quad (55) \end{aligned}$$

for some  $\beta(\alpha^*), \sigma(\alpha^*) \in \mathbb{R}_{>0}$ .

*Proof.* It follows from standard semigroup arguments for semilinear problems (see, e.g., Theorem 11.1.5 in Curtain and Zwart (2020) or 6.1.4 in Pazy (1983)) that the closed-loop ODE-PDE interconnection (38) admits a unique local mild solution  $(X_\delta, \zeta) \in C^0([0, t_{\max}); \mathcal{X})$  for all ICs  $(X_{\delta,0}, \zeta_0) \triangleq (X_\delta(0), \zeta(0, 0)) \in \mathcal{X}$ . Consequently, from the transformations  $X(t) \triangleq X_\delta(t) + X^*$  and  $z(\xi, t) \triangleq \zeta(\xi, t) + \varphi(\xi, \alpha(X(t), U(t)))$ , with  $U(t) = U^*$  and  $\varphi(\cdot, \alpha(X(t), U(t))) \in \mathcal{D}(\mathcal{A})$ , it may be concluded the original ODE-PDE interconnection (8) also admits a unique mild solution  $(X, z) \in C^0([0, t_{\max}); \mathcal{X})$  for all ICs  $(X_0, z_0) \in \mathcal{X}$ . Moreover, according to Theorem 2.1, to prove global well-posedness, it is sufficient to show that  $\|(X(t), z(\cdot, t))\|_{\mathcal{X}} < \infty$  for all  $t \in \mathbb{R}_{\geq 0}$ , which is implied by inequality (54) under Assumption 2.3. In particular, for sufficiently regular solutions, an application of Grönwall-Bellman's inequality, in conjunction with the fact that

the Lyapunov function  $V(X_\delta(t), \zeta(\cdot, t))$  is equivalent to the squared norm  $\|(X_\delta(t), \zeta(\cdot, t))\|_{\mathcal{X}}^2$  on  $\mathcal{X}$ , yields

$$\begin{aligned} &\|(X_\delta(t), \zeta(\cdot, t))\|_{\mathcal{X}} \\ &\leq \beta(\alpha^*)e^{-\sigma(\alpha^*)t}\|(X_{\delta,0}, \zeta_0(\cdot))\|_{\mathcal{X}}, \quad t \in [0, T], \end{aligned} \quad (56)$$

which proves (55). The result may then be extended to mild solutions using standard density arguments.  $\square$

Before moving to the design of a stabilizing controller, some conclusive remarks are collected below.

**Remark 4.** *Typically,  $\bar{L} < 1$  is treated as a fixed parameter, whereas  $v_x$  may vary over a broad range. Consequently, the perturbation parameter  $\epsilon$  mostly depends on the vehicle's cruising speed. Therefore, Theorem 3.1 states that, for sufficiently small  $\epsilon$  (and thus high  $v_x$ ), the stability of the semilinear single-track models may be studied using standard finite-dimensional approaches. In contrast, at sufficiently low values of  $v_x$ ,  $\epsilon$  may approach unity, thereby invalidating the stability results derived from singular perturbation analysis. In particular, this happens at very low velocities, where the loss of time-scale separation can give rise to so-called micro-shimmy behaviors that models with static tires do not capture.*

A counterexample to the results of Proposition 3.1 is provided graphically in Figure 4, where a local stability chart is illustrated for a semilinear single-track vehicle model (8) with distributed tires, using typical parameter values (Romano, Aamo, Åslund, et al. 2026b). The chart, produced using spectral methods, reveals the existence of unstable islands in understeer vehicles ( $\tilde{C}_1(0)l_1 < \tilde{C}_2(0)l_2$ ) for sufficiently low values of the longitudinal speed  $v_x$ . As discussed in Takács and Stépán (2013), Romano, Aamo, Åslund, et al. (2024), and Romano, Aamo, Åslund, et al. (2026b), the unstable regions in Figure 4 are associated with micro-shimmy oscillations and are not predicted by the reduced order model (30).

## 4 Stabilization

Single-track vehicle models – especially *oversteer* ones – might be unstable. Therefore, the present section is dedicated to the synthesis of state and output-feedback controllers that (locally) exponentially stabilize (8) around a desired equilibrium  $X^* \in \mathbb{R}^2$  as in (24), corresponding to a stationary input  $U(t) = U^*$ . Specifically, a state-feedback control law is designed in Section 4.1, whereas the output-feedback case is addressed in Section 4.2.

### 4.1 State-feedback stabilization

A state-feedback stabilizing controller is first synthesized in Section 4.1.1 via singular perturbation analysis. Section 4.1.2 works out the extension for sufficiently small values of the parameter  $\epsilon$ .

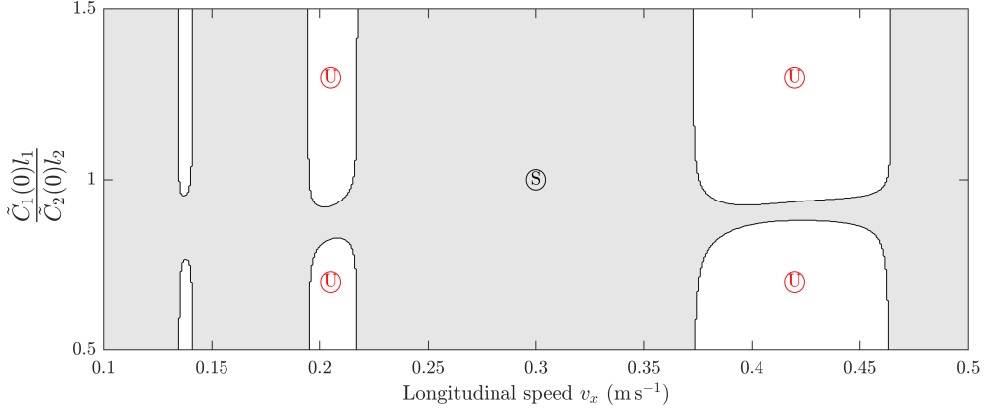


Figure 4: Local stability chart for a semilinear single-track vehicle model (8) with constant pressure distribution and flexible tire carcass (Parametrization 2.2) with  $b = 0$ , linearized around the zero equilibrium  $(X^*, z^*(\xi), U^*) = (0, 0, 0)$ , for different values of the understeer index  $\frac{C_1(0)l_1}{C_2(0)l_2}$  and longitudinal speed  $v_x$ . The unstable regions (in white) correspond to combinations of parameters associated with micro-shimmy oscillations that are not detected by reduced order representations. Model parameters as in Romano, Aamo, Åslund, et al. (2026b).

#### 4.1.1 Analysis via singular perturbation theory

Repeating analogous calculations as in Section 3.1.1 and specifying the input as  $\bar{U}(t) = U^* + \bar{U}_\delta(t)$ , with

$$\bar{U}_\delta(t) = F(\alpha^*)\bar{X}_\delta(t), \quad (57)$$

where  $F(\alpha^*) \in \mathbf{M}_2(\mathbb{R})$  is a matrix to be appropriately selected, produces, after an exact first-order Taylor's expansion,

$$\dot{\bar{X}}_\delta(t) = \tilde{A}_1^*(\alpha^*)\bar{X}_\delta(t) + R^*(\bar{X}_\delta(t), \alpha^*), \quad t \in (0, T), \quad (58)$$

where the matrix  $\tilde{A}_1^*(\alpha^*) \in \mathbf{M}_2(\mathbb{R})$  is defined as

$$\tilde{A}_1^*(\alpha^*) \triangleq \tilde{A}_1(\alpha^*) + \tilde{G}_1(\alpha^*)F(\alpha^*), \quad (59)$$

and, for every  $\alpha^* \in \mathbb{R}^2$ ,  $R^*(\cdot, \alpha^*) \in C^0(\mathbb{R}^2; \mathbb{R}^2)$  satisfies

$$\lim_{\|Z\|_2 \rightarrow 0} \frac{\|R^*(Z, \alpha^*)\|_2}{\|Z\|_2} = 0. \quad (60)$$

Local exponential stability results for the closed-loop reduced ODE subsystem (58) are asserted by Proposition 4.1 below.

**Proposition 4.1.** *Under Assumptions 2.3 and 2.4, consider the reduced ODE subsystem (58) along with the equilibrium  $(X^*, U^*)$ , and the control law  $\bar{U}(t) = U^* + \bar{U}_\delta(t)$ , with  $\bar{U}_\delta(t)$  as in (57) and the gain  $F(\alpha^*) \in \mathbf{M}_2(\mathbb{R})$  designed such that the matrix  $\tilde{A}_1^*(\alpha^*) \in \mathbf{M}_2(\mathbb{R})$  in (59) is Hurwitz. Then, there exists  $r^* \in \mathbb{R}_{>0}$  such that, for all ICs  $\bar{X}_0 \triangleq \bar{X}(0) \in \mathbb{R}^2$  with  $\|\bar{X}_0 - X^*\|_2 < r^*$ , the unique solution  $\bar{X} \in C^0(\mathbb{R}_{\geq 0}; \mathbb{R}^2)$  to (58) satisfies*

$$\|\bar{X}(t) - X^*\|_2 \leq \beta_1^*(\alpha^*)e^{-\sigma_1^*(\alpha^*)t}\|\bar{X}_0 - X^*\|_2, \quad t \in [0, T], \quad (61)$$

for some  $\beta_1^*(\alpha^*), \sigma_1^*(\alpha^*) \in \mathbb{R}_{>0}$ .

The boundary layer PDE subsystem is still given by (36).

#### 4.1.2 Stability analysis for sufficiently small $\epsilon$

Inspired by the analysis conducted in the previous Section 4.1.1, the control law is specified as  $U(t) = U^* + U_\delta(t)$ , with  $U_\delta(t) \in \mathbb{R}^2$  given by

$$U_\delta(t) = F(\alpha^*)X_\delta(t). \quad (62)$$

With the above control law (62), the ODE-PDE interconnection (8) may be recast as

$$\begin{aligned} \dot{X}_\delta(t) &= \tilde{A}_1^*(\alpha^*)X_\delta(t) + R^*(X_\delta(t), \alpha^*) + G_1(\mathcal{K}_1\zeta)(t) \\ &\quad + G_1\Sigma(\alpha(X(t), U^*))( \mathcal{K}_2\zeta)(t), \quad t \in (0, T), \end{aligned}$$

$$\frac{\partial \zeta(\xi, t)}{\partial t} + \frac{\Lambda}{\epsilon} \frac{\partial \zeta(\xi, t)}{\partial \xi} = \frac{1}{\epsilon} \Sigma(\alpha(X(t), U(t))) \quad (63a)$$

$$\begin{aligned} &\times [\zeta(\xi, t) + (\mathcal{K}_3\zeta)(t)] + \frac{1}{\epsilon}(\mathcal{K}_4\zeta)(t) \\ &- \frac{\partial \varphi(\xi, \alpha(X(t), U(t)))}{\partial \alpha} (A_2 + G_2F(\alpha^*)) \\ &\times [\tilde{A}_1^*(\alpha^*)X_\delta(t) + R^*(X_\delta(t), \alpha^*) + G_1(\mathcal{K}_1\zeta)(t)] \\ &- \frac{\partial \varphi(\xi, \alpha(X(t), U(t)))}{\partial \alpha} (A_2 + G_2F(\alpha^*)) \\ &\times G_1\Sigma(\alpha(X(t), U(t)))(\mathcal{K}_2\zeta)(t), \quad (\xi, t) \in (0, 1) \times (0, T), \end{aligned} \quad (63b)$$

$$\zeta(0, t) = 0, \quad t \in (0, T), \quad (63c)$$

Theorem 4.1 below represents the state-feedback counterpart of Theorem 3.1.

**Theorem 4.1.** *Under Assumptions 2.1-2.4, consider the ODE-PDE interconnection (8) along with the equilibrium  $(X^*, U^*)$ , and the control law  $U(t) = U^* + U_\delta(t)$ , with  $U_\delta(t)$*

as in (62) and the gain  $F(\alpha^*) \in \mathbf{M}_2(\mathbb{R})$  designed such that the matrix  $\tilde{A}_1^*(\alpha^*) \in \mathbf{M}_2(\mathbb{R})$  in (59) is Hurwitz. Then, there exist  $\epsilon^{**}(\alpha^*), r_\epsilon^*(\alpha^*) \in \mathbb{R}_{>0}$  such that, for all  $\epsilon \in (0, \epsilon^{**}(\alpha^*))$  and ICs  $(X_0, z_0(\cdot)) \in \mathcal{X}$  verifying  $\|(X_0 - X^*, \zeta_0(\cdot))\|_{\mathcal{X}} < r_\epsilon^*(\alpha^*)$ , the ODE-PDE system (8) admits a unique mild solution  $(X, z) \in C^0(\mathbb{R}_{\geq 0}; \mathcal{X})$  satisfying

$$\begin{aligned} & \|(X(t) - X^*, \zeta(\cdot, t))\|_{\mathcal{X}} \\ & \leq \beta^*(\alpha^*) e^{-\sigma^*(\alpha^*)t} \|(X_0 - X^*, \zeta_0(\cdot))\|_{\mathcal{X}}, \quad t \in [0, T], \end{aligned} \quad (64)$$

for some  $\beta^*(\alpha^*), \sigma^*(\alpha^*) \in \mathbb{R}_{>0}$ .

*Proof.* The proof is similar to that of Theorem 3.1, and thus omitted.  $\square$

Theorem 4.1 provides a systematic way to stabilize the semilinear single-track model via state-feedback control. In reality, measurements of the lateral velocity  $v_y(t)$  are not commonly available, which motivates the design of an output-feedback controller, as addressed next in Section 4.2.

## 4.2 Output-feedback stabilization

An output-feedback stabilizing controller is first synthesized in Section 4.2.1 via singular perturbation analysis. Section 4.2.2 works out the extension for sufficiently small values of the parameter  $\epsilon$ .

### 4.2.1 Analysis via singular perturbation theory

Denoting with  $\hat{X}(t) \in \mathbb{R}^2$  and  $\hat{Y}(t) \in \mathbb{R}$  the estimates of  $X(t)$  and  $Y(t)$ , respectively, the following observer structure is proposed:

$$\begin{aligned} \dot{\hat{X}}(t) &= A_1 \hat{X}(t) + G_1 \Phi(\alpha(\hat{X}(t), U(t))) \\ &+ b - L(\alpha^*)(Y(t) - \hat{Y}(t)), \quad t \in (0, T), \end{aligned} \quad (65)$$

where  $L(\alpha^*) \in \mathbf{M}_{2 \times 1}(\mathbb{R})$  is a matrix to be appropriately selected.

Defining  $\mathbb{R}^2 \ni \tilde{X}(t) \triangleq X(t) - \hat{X}(t)$  and  $\mathbb{R} \ni \tilde{Y}(t) \triangleq Y(t) - \hat{Y}(t)$  and subtracting (65) from (8a) provides

$$\begin{aligned} \dot{\tilde{X}}(t) &= A_1 \tilde{X}(t) + G_1 \left[ (\mathcal{H}_1 z)(t) + \Sigma(\alpha(X(t), U(t)))(\mathcal{H}_2 z)(t) \right. \\ &+ G_1 h_1(\alpha(X(t), U(t))) - G_1 \Phi(\alpha(\hat{X}(t), U(t))) \\ &+ L(\alpha^*) \tilde{Y}(t), \quad t \in (0, T). \end{aligned} \quad (66)$$

Inserting (29) into (66) yields

$$\begin{aligned} \dot{\tilde{X}}(t) &= A_1 \tilde{X}(t) + G_1 \Phi(\alpha(\tilde{X}(t), \bar{U}(t))) \\ &- G_1 \Phi(\alpha(\tilde{X}(t), \bar{U}(t))) + L(\alpha^*) C \tilde{X}(t), \quad t \in (0, T), \end{aligned} \quad (67)$$

where the bar notation has again been adopted to indicate the variables corresponding to  $\epsilon = 0$ . Hence, decomposing again  $\bar{U}(t) = U^* + \bar{U}_\delta(t)$  and specifying the control law  $\bar{U}_\delta(t)$  as

$$\bar{U}_\delta(t) = F(\alpha^*)(\tilde{X}(t) - X^*) \quad (68)$$

gives, after performing an exact first-order Taylor's expansion around  $(X^*, 0) \in \mathbb{R}^4$ ,

$$\begin{bmatrix} \dot{\tilde{X}}_\delta(t) \\ \dot{\tilde{X}}(t) \end{bmatrix} = \tilde{A}^*(\alpha^*) \begin{bmatrix} \tilde{X}_\delta(t) \\ \tilde{X}(t) \end{bmatrix} + \bar{R} \left( (\tilde{X}_\delta(t), \tilde{X}(t)), \alpha^* \right), \quad t \in (0, T), \quad (69)$$

where  $\tilde{A}^*(\alpha^*) \in \mathbf{M}_4(\mathbb{R})$  is given by

$$\tilde{A}^*(\alpha^*) = \begin{bmatrix} \tilde{A}_1^*(\alpha^*) & \tilde{A}_2^*(\alpha^*) \\ 0 & \tilde{A}_3^*(\alpha^*) \end{bmatrix}, \quad (70)$$

with  $\tilde{A}_1^*(\alpha^*) \in \mathbf{M}_2(\mathbb{R})$  reading according to (59), and  $\tilde{A}_2^*(\alpha^*), \tilde{A}_3^*(\alpha^*) \in \mathbf{M}_2(\mathbb{R})$  defined as

$$\tilde{A}_2^*(\alpha^*) \triangleq -G_1 \tilde{C}(\alpha^*) G_2 F(\alpha^*), \quad (71a)$$

$$\tilde{A}_3^*(\alpha^*) \triangleq A_1 + G_1 \tilde{C}(\alpha^*) A_2 + L(\alpha^*) C, \quad (71b)$$

and

$$\bar{R} \left( (\tilde{X}_\delta(t), \tilde{X}(t)), \alpha^* \right) = \begin{bmatrix} \bar{R}_1 \left( (\tilde{X}_\delta(t), \tilde{X}(t)), \alpha^* \right) \\ \bar{R}_2 \left( (\tilde{X}_\delta(t), \tilde{X}(t)), \alpha^* \right) \end{bmatrix}. \quad (72)$$

For every  $\alpha^* \in \mathbb{R}^2$ , the function  $\bar{R}(\cdot, \alpha^*) \in C^0(\mathbb{R}^4; \mathbb{R}^4)$  appearing in (69) satisfies

$$\lim_{\|Z\|_2 \rightarrow 0} \frac{\|\bar{R}(Z, \alpha^*)\|_2}{\|Z\|_2} = 0. \quad (73)$$

Exploiting the upper-triangular structure of the matrix  $\tilde{A}^*(\alpha^*)$  in (70), the following result is promptly obtained.

**Proposition 4.2.** *Under Assumptions 2.3, 2.4, and 2.5, consider the reduced ODE subsystem (69) along with the equilibrium  $(X^*, U^*)$ , and the control law  $\bar{U}(t) = U^* + \bar{U}_\delta(t)$ , with  $\bar{U}_\delta(t)$  as in (68) and the gains  $F(\alpha^*) \in \mathbf{M}_2(\mathbb{R})$  and  $L(\alpha^*) \in \mathbf{M}_{2 \times 1}(\mathbb{R})$  designed such that the matrix  $\tilde{A}^*(\alpha^*) \in \mathbf{M}_4(\mathbb{R})$  in (70) is Hurwitz. Then, there exists  $\bar{r} \in \mathbb{R}_{>0}$  such that, for all ICs  $(\tilde{X}_0, \tilde{X}_0) \triangleq (\tilde{X}(0), \tilde{X}(0)) \in \mathbb{R}^4$  with  $\|(\tilde{X}_0 - X^*, \tilde{X}_0)\|_2 < \bar{r}$ , the unique solution  $(\tilde{X}, \tilde{X}) \in C^0(\mathbb{R}_{\geq 0}; \mathbb{R}^4)$  to (69) satisfies*

$$\begin{aligned} & \|(X(t) - X^*, \tilde{X}(t))\|_2 \\ & \leq \bar{\beta}_1(\alpha^*) e^{-\bar{\sigma}_1(\alpha^*)t} \|(X_0 - X^*, \tilde{X}_0)\|_2, \quad t \in [0, T], \end{aligned} \quad (74)$$

for some  $\bar{\beta}_1(\alpha^*), \bar{\sigma}_1(\alpha^*) \in \mathbb{R}_{>0}$ .

The boundary layer PDE subsystem is still given by (36).

### 4.2.2 Stability analysis for sufficiently small $\epsilon$

Inspired by the analysis conducted in the previous Section 4.2.1, the control law is specified as  $U(t) = U^* + U_\delta(t)$ , with  $U_\delta(t) \in \mathbb{R}^2$  given by

$$U_\delta(t) = F(\alpha^*)(\hat{X}(t) - X^*). \quad (75)$$

With the above control law (62), the ODE-PDE interconnection (8) with the observer (65) may be recast as

$$\begin{bmatrix} \dot{\bar{X}}_\delta(t) \\ \dot{\tilde{X}}(t) \end{bmatrix} = \tilde{A}^*(\alpha^*) \begin{bmatrix} \bar{X}_\delta(t) \\ \tilde{X}(t) \end{bmatrix} + \bar{R} \left( \left( \bar{X}_\delta(t), \tilde{X}(t) \right), \alpha^* \right) \\ + \begin{bmatrix} I_2 \\ I_2 \end{bmatrix} G_1 \left[ (\mathcal{K}_1 \zeta)(t) + \Sigma(\alpha(X(t), U(t))) (\mathcal{K}_2 \zeta)(t) \right], \\ t \in (0, T), \quad (76a)$$

$$\begin{aligned} \frac{\partial \zeta(\xi, t)}{\partial t} + \frac{A}{\epsilon} \frac{\partial \zeta(\xi, t)}{\partial \xi} &= \frac{1}{\epsilon} \Sigma(\alpha(X(t), U(t))) \\ &\times [\zeta(\xi, t) + (\mathcal{K}_3 \zeta)(t)] + \frac{1}{\epsilon} (\mathcal{K}_4 \zeta)(t) \\ &- \frac{\partial \varphi(\xi, \alpha(X(t), U(t)))}{\partial \alpha} (A_2 + G_2 F(\alpha^*)) \\ &\times [\tilde{A}_1^*(\alpha^*) \bar{X}_\delta(t) + \tilde{A}_2^*(\alpha^*) \tilde{X}(t) + \bar{R}_1((X_\delta(t), \tilde{X}(t)), \alpha^*)] \\ &+ \frac{\partial \varphi(\xi, \alpha(X(t), U(t)))}{\partial \alpha} G_2 F(\alpha^*) \\ &\times [\tilde{A}_3^*(\alpha^*) \tilde{X}(t) + \bar{R}_2((X_\delta(t), \tilde{X}(t)), \alpha^*)] \\ &- \frac{\partial \varphi(\xi, \alpha(X(t), U(t)))}{\partial \alpha} A_2 \\ &\times G_1 \left[ (\mathcal{K}_1 \zeta)(t) + \Sigma(\alpha(X(t), U(t))) (\mathcal{K}_2 \zeta)(t) \right], \\ &(\xi, t) \in (0, 1) \times (0, T), \quad (76b) \end{aligned}$$

$$\zeta(0, t) = 0, \quad t \in (0, T). \quad (76c)$$

Utilizing the ODE-PDE system (76), and resorting to similar arguments as those adopted in Section 3.2, it is straightforward to deduce the final result of the paper, formalized in Theorem 4.2.

**Theorem 4.2.** *Under Assumptions 2.1-2.5, consider the ODE-PDE interconnection (8) along with the equilibrium  $(X^*, U^*)$ , the observer (65), and the control law  $U(t) = U^* + U_\delta(t)$ , with  $U_\delta(t)$  as in (75) and the gains  $F(\alpha^*) \in \mathbf{M}_2(\mathbb{R})$  and  $L(\alpha^*) \in \mathbf{M}_{2 \times 1}(\mathbb{R})$  designed such that the matrix  $\tilde{A}^*(\alpha^*) \in \mathbf{M}_4(\mathbb{R})$  in (70) is Hurwitz. Then, there exist  $\bar{\epsilon}^*(\alpha^*)$ ,  $\bar{r}_\epsilon(\alpha^*) \in \mathbb{R}_{>0}$  such that, for all  $\epsilon \in (0, \bar{\epsilon}^*(\alpha^*))$  and ICs  $(X_0, z_0(\cdot), \tilde{X}_0) \triangleq (X(0), z(\cdot, 0), \tilde{X}(0)) \in \mathcal{X} \times \mathbb{R}^2$  verifying  $\|(X_0 - X^*, z_0(\cdot), \tilde{X}_0)\|_{\mathcal{X} \times \mathbb{R}^2} < \bar{r}_\epsilon(\alpha^*)$ , the ODE-PDE system (8) admits a unique mild solution  $(X, z, \tilde{X}) \in C^0(\mathbb{R}_{\geq 0}; \mathcal{X} \times \mathbb{R}^2)$  satisfying*

$$\begin{aligned} &\|(X(t) - X^*, z(\cdot, t), \tilde{X}(t))\|_{\mathcal{X} \times \mathbb{R}^2} \\ &\leq \bar{\beta}(\alpha^*) e^{-\bar{\sigma}(\alpha^*) t} \|(X_0 - X^*, z_0(\cdot), \tilde{X}_0)\|_{\mathcal{X} \times \mathbb{R}^2}, \quad t \in [0, T], \quad (77) \end{aligned}$$

for some  $\bar{\beta}(\alpha^*)$ ,  $\bar{\sigma}(\alpha^*) \in \mathbb{R}_{>0}$ .

*Proof.* The proof is similar to that of Theorem 3.1, and thus omitted.  $\square$

Before discussing some numerical simulations, the concluding remarks are summarized below.

**Remark 5.** *Theorems 4.1 and 4.2 state that, for sufficiently small  $\epsilon$  (or, equivalently, high longitudinal speeds  $v_x$ ), state and output-feedback stabilizing controllers can be designed based solely on the reduced order single-track vehicle models obtained by disregarding the transient tire dynamics. This is the standard approach in the literature, but it has never been justified rigorously before.*

## 5 Simulation results

The numerical values for the model parameters of the example discussed below are listed in Table 1. With the given combination of parameters, Assumptions 2.1-2.5 are all fulfilled. Moreover, the considered vehicle is oversteer, and hence inherently unstable for values of the longitudinal speed beyond a critical value.

In this context, the following numerical results refer to simulations conducted in MATLAB/Simulink® environment. The semilinear PDE subsystem was solved numerically using a finite difference scheme with a discretization step of 0.02, and combined with a time-marching algorithm with a fixed time step of  $10^{-6}$  s. The ICs for the actual system were set to  $X_0 = [0.03 \ -0.25]^T$ , and  $z_0(\xi) = [0.027 \ 0.033]^T$  (corresponding to  $\|z_0(\cdot)\|_{L^2((0,1); \mathbb{R}^2)} = 0.043$ ), whereas those for the observer to  $\hat{X}_0 = [0 \ 0]^T$ . A control input delay of  $\delta_U = 0.02$  s was introduced, and the yaw rate measurements were corrupted with additive white noise having a standard deviation of  $0.1 \text{ rad s}^{-1}$  and a sample time of 0.005 s, which reflects the noise level typically observed in standard automotive sensors.

Figure 5 illustrates the unstable behavior of the uncontrolled vehicle driving at  $v_x = 50 \text{ m s}^{-1}$ . The semilinear observer synthesized as in Section 4.2, with  $L \in \mathbf{M}_{2 \times 1}(\mathbb{R})$  in (65) specified as

$$L = \begin{bmatrix} -16.02 \\ -147.267 \end{bmatrix}, \quad (78)$$

predicts the true states with great accuracy, with the estimates converging approximately for  $t = 3$  s.

The closed loop trends of the kinematic variables, axle forces, and steering inputs obtained by setting

$$F = \begin{bmatrix} 2.034 & -0.0458 \\ 0 & 0 \end{bmatrix}, \quad (79)$$

are depicted in Figure 6(a), (b), and (c), where a rapid convergence around zero may be observed concerning all the involved quantities, with small sustained oscillations caused by the noisy measurement. In particular, the steering angle  $\delta_1(t)$  initially exhibits a pronounced transient, but never exceeds  $4^\circ$  in absolute value, confirming *a posteriori* the feasibility of the maneuver.

Similar considerations may be drawn by inspecting Figure 7, where closed loop dynamics of the PDE states  $\zeta(\xi, t)$

Parameter	Description	Unit	Value
$v_x$	Longitudinal speed	$\text{m s}^{-1}$	50
$m$	Vehicle mass	kg	1300
$I_z$	Vertical moment of inertia	$\text{kg m}^2$	2000
$l_1$	Front axle length	m	1.4
$l_2$	Rear axle length	m	1
$F_{z1}$	Front vertical force	N	$2.66 \cdot 10^3$
$F_{z2}$	Rear vertical force	N	$3.72 \cdot 10^3$
$F_w$	Lateral wind force	N	0
$l_w$	Wind force offset	m	0
$L_1$	Front contact patch length	m	0.11
$L_2$	Rear contact patch length	m	0.09
$\sigma_{0,1}$	Front micro-stiffness	$\text{m}^{-1}$	240
$\sigma_{0,2}$	Rear micro-stiffness	$\text{m}^{-1}$	269
$\phi_1$	Front structural parameter	-	0.92
$\phi_2$	Rear structural parameter	-	0.92
$\bar{\mu}_1(\cdot)$	Front friction coefficient	-	1
$\bar{\mu}_2(\cdot)$	Rear friction coefficient	-	1
$\bar{g}_1(\cdot)$	Front friction function	-	1
$\bar{g}_2(\cdot)$	Rear friction function	-	1
$\chi$	Rear steering actuation	-	0
$\varepsilon$	Regularization parameter	-	0

Table 1: Model parameters

are illustrated. Specifically, it may be observed that, under the action of the control input (75), the distributed states quickly approach zero, which is consistent with the observations reported above. Also in this case, residual oscillations of the state  $\zeta_1(\xi, t)$  should be ascribed to the noisy measurements, which affect the quality of the estimates and desired forces. Additional simulations were conducted by slightly varying the controller and observer gains, without appreciable differences in the qualitative behavior of the closed-loop system.

The results asserted by Theorem 4.2 are of a local nature: ICs deviating largely from the target equilibrium may destabilize the closed loop system's response. Additionally, relatively large values of the parameter  $\epsilon$  – which is essentially determined by the longitudinal speed  $v_x$  for constant  $L_1$  and  $L_2$  – may invalidate the conclusion of the singular perturbation analysis. In this context, the influence of different initial conditions  $X_0 = -k[0.03 - 0.05]^\top$  on the closed loop dynamics of the ODE-PDE system is illustrated in Figure 8 for  $k = 1, 3$ , and  $6$ . As intuitively expected, ICs that are further from the target equilibrium may slow down the convergence of the norm  $\|(X(t) - X^*, \zeta(\cdot, t), \hat{X}(t))\|_{\mathcal{X} \times \mathbb{R}^2}$ , which is particularly noticeable for  $k = 6$ . Finally, the effect of different values of  $v_x = 10, 20$ , and  $50 \text{ m s}^{-1}$  is investigated

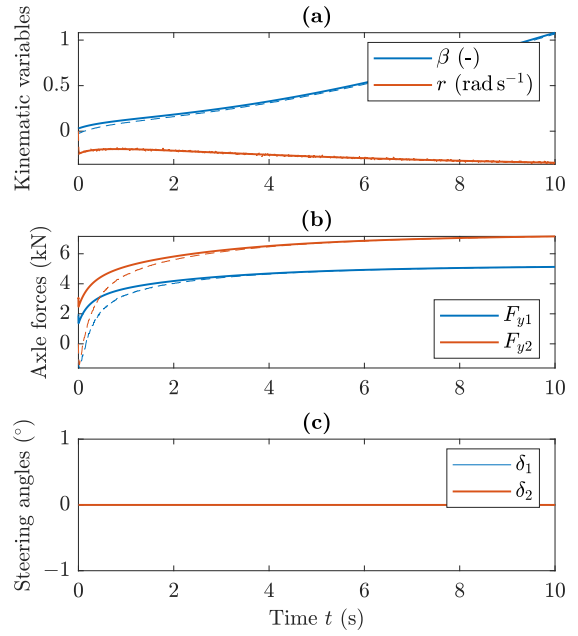


Figure 5: Open loop behavior of the lumped states and steering inputs, for  $L$  as in (78): (a) kinematic variables; (b) axle forces; (c) steering inputs.

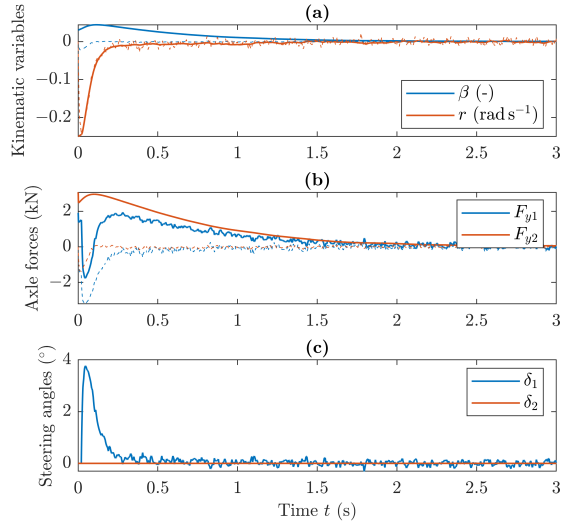


Figure 6: Closed loop behavior of the lumped states and steering inputs, for  $L$  and  $F$  as in (78) and (79), respectively: (a) kinematic variables; (b) axle forces; (c) steering inputs.

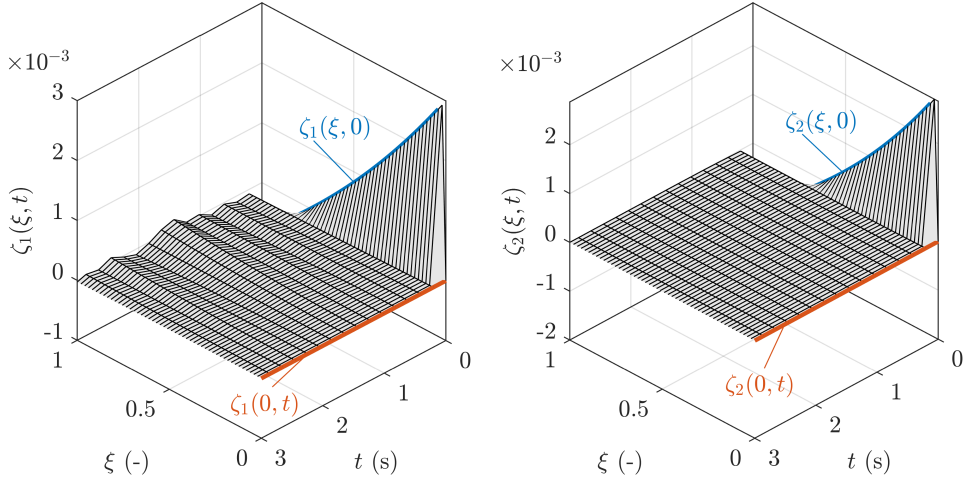


Figure 7: Evolution of the PDE states  $\zeta(\xi, t)$ , along with its IC (blue lines) and BC (orange lines).

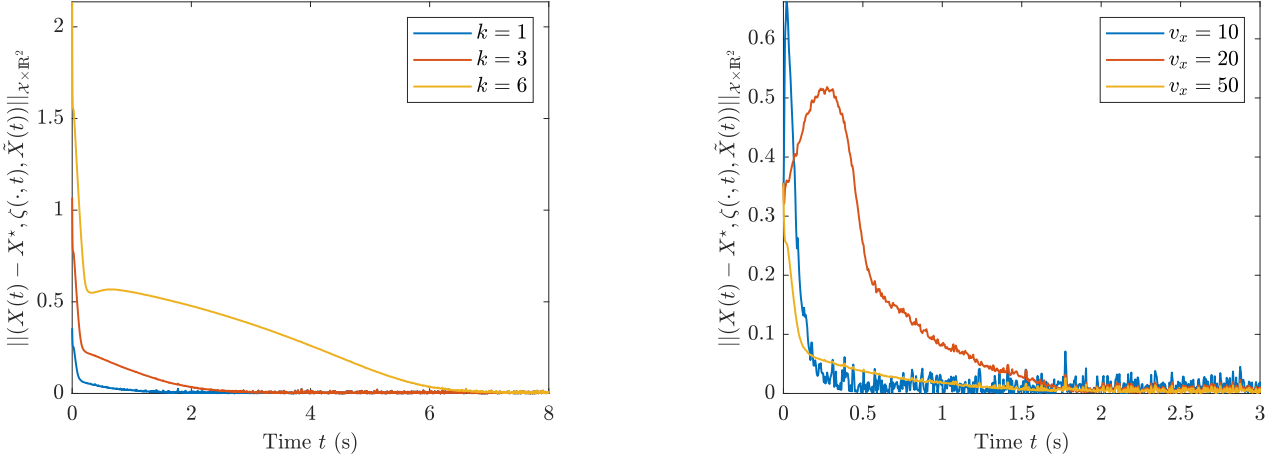


Figure 8: Closed loop behavior of  $\|(X(t) - X^*, \zeta(\cdot, t), \tilde{X}(t))\|_{X \times \mathbb{R}^2}$  for different values of  $k = 1, 3$ , and  $6$ .

graphically in Figure 9, which demonstrates that the synthesized controller can successfully stabilize the ODE-PDE interconnection (8) on a wide range of longitudinal speeds.

## 6 Conclusions

The present paper investigated the stability and stabilization of semilinear single-track vehicle models with distributed tire friction dynamics using singular perturbation analysis. Specifically, it was shown that when an appropriate perturbation parameter – defined as the ratio between a characteristic length scale of the rolling contact problem and the vehicle’s longitudinal speed – is sufficiently small, standard finite-dimensional methods can successfully be applied to study the local stability of system equilibria and to design stabilizing state- and output-feedback controllers. Whilst the paper’s results do not introduce new observer

Figure 9: Closed loop behavior of  $\|(X(t) - X^*, \zeta(\cdot, t), \tilde{X}(t))\|_{X \times \mathbb{R}^2}$  for different values of  $v_x = 10, 20$ , and  $50 \text{ m s}^{-1}$ .

or controller design strategies, they provide the first rigorous mathematical justification for long-standing practices in automotive research, establishing fundamental advances in vehicle dynamics and opening new perspectives for the control of semilinear ODE-PDE systems with distributed friction.

Future research will explore the design of nonlinear controllers, possibly in conjunction with adaptive observers for vehicle state and friction estimation, along with their impact on the dynamics of the full ODE-PDE interconnection. Additionally, the behavior of more complex vehicle models, incorporating the effect of large steering angles and suspension dynamics, should be studied.

## Acknowledgments

This research was financially supported by the project FASTEST (Reg. no. 2023-06511), funded by the Swedish Research Council.

## Declaration of interest

Declaration of interest: none.

## References

Anfinsen, H. and O. M. Aamo (2019). *Adaptive Control of Hyperbolic PDEs*. Cham: Springer.

Bastin, G. and J.-M. Coron (2016). *Stability and Boundary Stabilization of 1-D Hyperbolic Systems*. Cham: Birkhäuser. DOI: [10.1007/978-3-319-32062-5](https://doi.org/10.1007/978-3-319-32062-5).

Beregi, S., D. Takács, and G. Gyebroszki (2019). “Theoretical and experimental study on the nonlinear dynamics of wheel-shimmy”. In: *Nonlinear Dyn.* 98, pp. 2581–2593. DOI: [10.1007/s11071-019-05225-w](https://doi.org/10.1007/s11071-019-05225-w).

Beregi, S., D. Takács, and G. Stépán (2016). “Tyre induced vibrations of the car-trailer system”. In: *J. Sound Vib.* 362, pp. 215–227.

Canudas-de-Wit, C. and P. Tsotras (1999). “Dynamic tire friction models for vehicle traction control”. In: *Proc. IEEE Conf. Decis. Control*, pp. 3746–3751. DOI: [10.1109/CDC.1999.827937](https://doi.org/10.1109/CDC.1999.827937).

Canudas-de-Wit, C., P. Tsotras, and E. Velenis (2003). “Dynamic Friction Models for Road/Tire Longitudinal Interaction”. In: *Veh. Syst. Dyn.* 39.3, pp. 189–226.

Cerpa, E. and C. Prieur (2017). “Effect of time scales on stability of coupled systems involving the wave equation”. In: *Proc. IEEE Conf. Decis. Control*, pp. 1236–1241. DOI: [10.1109/CDC.2017.8263825](https://doi.org/10.1109/CDC.2017.8263825).

Curtain, R. and H. Zwart (2020). *Introduction to Infinite-Dimensional Systems Theory: A State-Space Approach*. 1st ed. New York: Springer.

Deur, J. (2001). “Modeling and Analysis of Longitudinal Tire Dynamics Based on the LuGre Friction Model”. In: *IFAC Proc. Vol.* 34.1, pp. 91–96. DOI: [10.1016/S1474-6670\(17\)34383-5](https://doi.org/10.1016/S1474-6670(17)34383-5).

Deur, J., J. Asgari, and D. Hrovat (2004). “A 3D Brush-type Dynamic Tire Friction Model”. In: *Veh. Syst. Dyn.* 42.3, pp. 133–173.

Deur, J., V. Ivanović, and M. Troulis (2005). “Extensions of the LuGre tyre friction model related to variable slip speed along the contact patch length”. In: *Veh. Syst. Dyn.* 43, pp. 508–524.

Du, H., N. Zhang, and G. Dong (2010). “Stabilizing Vehicle Lateral Dynamics With Considerations of Parameter Uncertainties and Control Saturation Through Robust Yaw Control”. In: *IEEE Transactions on Vehicular Technology* 59.5, pp. 2593–2597. DOI: [10.1109/TVT.2010.2045520](https://doi.org/10.1109/TVT.2010.2045520).

Guiggiani, M. (2023). *The Science of Vehicle Dynamics*. 3rd ed. Cham: Springer. DOI: [10.1007/978-3-031-06461-6](https://doi.org/10.1007/978-3-031-06461-6).

Guo, N. et al. (2021). “A supervisory control strategy of distributed drive electric vehicles for coordinating handling, lateral stability, and energy efficiency”. In: *IEEE Transactions on Transportation Electrification* 7.4, pp. 2488–2504.

Krstić, M. and A. Smyshlyaev (2008). *Boundary Control of PDEs: A Course on Backstepping Designs*. SIAM.

Lenzo, B., M. Zanchetta, and A. Sorniotti (2020). “Yaw Rate and Sideslip Angle Control Through Single Input Single Output Direct Yaw Moment Control”. In: *IEEE Transactions on Control Systems Technology*.

Li, Z. et al. (2022). “Integrated Longitudinal and Lateral Vehicle Stability Control for Extreme Conditions With Safety Dynamic Requirements Analysis”. In: *IEEE Transactions on Intelligent Transportation Systems* 23.10, pp. 19285–19298. DOI: [10.1109/TITS.2022.3152485](https://doi.org/10.1109/TITS.2022.3152485).

Markolefas, S., M. Guiggiani, and S. Georgantzinos (2024). “A general nonlinear single-track model for curved flat or banked road paths: Identification of the vehicle handling DNA”. In: *Int. J. Non-Linear Mech.* 166, p. 104850. DOI: [10.1016/j.ijnonlinmec.2024.104850](https://doi.org/10.1016/j.ijnonlinmec.2024.104850).

Nam, K., H. Fujimoto, and Y. Hori (2012). “Lateral Stability Control of In-Wheel-Motor-Driven Electric Vehicles Based on Sideslip Angle Estimation Using Lateral Tire Force Sensors”. In: *IEEE Transactions on Vehicular Technology* 61.5, pp. 1972–1985. DOI: [10.1109/TVT.2012.2191627](https://doi.org/10.1109/TVT.2012.2191627).

Pacejka, H. B. (2012). *Tire and Vehicle Dynamics*. 3rd ed. Amsterdam: Elsevier Butterworth-Heinemann.

Pazy, A. (1983). *Semigroups of Linear Operators and Applications to Partial Differential Equations*. New York: Springer. DOI: [10.1007/978-1-4612-5561-1](https://doi.org/10.1007/978-1-4612-5561-1).

Rill, G., T. Schaeffer, and M. Schuderer (2024). “LuGre or not LuGre”. In: *Multibody Syst. Dyn.* 60, pp. 191–218. DOI: [10.1007/s11044-023-09909-5](https://doi.org/10.1007/s11044-023-09909-5).

Romano, L. (2022). *Advanced Brush Tyre Modelling*. SpringerBriefs in Applied Sciences. Cham: Springer. DOI: [10.1007/978-3-030-98435-9](https://doi.org/10.1007/978-3-030-98435-9).

Romano, L., O. M. Aamo, J. Åslund, et al. (2024). “Stability analysis of linear single-track models with transient tyre dynamics”. In: *Veh. Syst. Dyn.*, pp. 1–35. DOI: [10.1080/00423114.2024.2445163](https://doi.org/10.1080/00423114.2024.2445163).

– (2025). “Stability and dissipativity of the distributed LuGre friction model”. In: *IEEE Control Syst. Lett.* DOI: [10.1109/LCSYS.2025.3572419](https://doi.org/10.1109/LCSYS.2025.3572419).

– (2026a). “First-order friction models with bristle dynamics: lumped and distributed formulations”. Submitted to *IEEE Trans. Control Syst. Technol.*

– (2026b). “Semilinear single-track models with distributed tyre friction dynamics”. In: *Nonlinear Dyn.* 114.138.

Romano, L., O. M. Aamo, M. Krstić, et al. (2025). “Passivity-exploiting stabilization of semilinear single-track vehicle models with distributed tire friction dynamics”. Under review at *Automatica*.

Schuderer, M., G. Rill, and T. Schaeffer (2025). “Friction modeling from a practical point of view”. In: *Multibody Syst. Dyn.* 63, pp. 141–158. DOI: [10.1007/s11044-024-09978-0](https://doi.org/10.1007/s11044-024-09978-0).

Shao, L. et al. (2016). “Nonlinear adaptive observer for side slip angle and road friction estimation”. In: *Proceedings of the IEEE Conference on Decision and Control*, pp. 6258–6265.

– (2019). “Robust road friction estimation during vehicle steering”. In: *Vehicle System Dynamics* 57.4, pp. 493–519.

Sharifzadeh, M., A. Akbari, et al. (2016). “Vehicle tyre/road interaction modeling and identification of its parameters using real-time trust-region methods”. In: *IFAC-PapersOnLine* 49.3, pp. 111–116. DOI: [10.1016/j.ifacol.2016.07.019](https://doi.org/10.1016/j.ifacol.2016.07.019).

Sharifzadeh, M., A. Senatore, et al. (2019). "A real-time approach to robust identification of tyre-road friction characteristics on mixed- $\mu$  roads". In: *Vehicle System Dynamics* 57.9, pp. 1338–1360. DOI: [10.1080/00423114.2018.1504974](https://doi.org/10.1080/00423114.2018.1504974).

Takács, D., G. Orosz, and G. Stépán (2009). "Delay effects in shimmy dynamics of wheels with stretched string-like tyres". In: *European Journal of Mechanics A/Solids* 28.3, pp. 516–525.

Takács, D. and G. Stépán (2012). "Micro-shimmy of towed structures in experimentally uncharted unstable parameter domain". In: *Vehicle System Dynamics* 50.11, pp. 1613–1630.

– (2013). "Contact patch memory of tyres leading to lateral vibrations of four-wheeled vehicles". In: *Philosophical Transactions of the Royal Society A* 371, p. 20120427. DOI: [10.1098/rsta.2012.0427](https://doi.org/10.1098/rsta.2012.0427).

Takács, D., G. Stépán, and S. J. Hogan (2008). "Isolated large amplitude periodic motions of towed rigid wheels". In: *Nonlinear Dynamics* 52, pp. 27–34. DOI: [10.1007/s11071-007-9253-y](https://doi.org/10.1007/s11071-007-9253-y).

Talbot, J., M. Brown, and J. C. Gerdes (2023). "Shared Control Up to the Limits of Vehicle Handling". In: *IEEE Transactions on Intelligent Vehicles* 9.1, pp. 2977–2987. DOI: [10.1109/TIV.2023.3300989](https://doi.org/10.1109/TIV.2023.3300989).

Tanelli, M., A. Astolfi, and S. M. Savaresi (2008). "Robust nonlinear output feedback control for brake by wire control systems". In: *Automatica* 44.4, pp. 1078–1087. DOI: [10.1016/j.automatica.2007.08.020](https://doi.org/10.1016/j.automatica.2007.08.020).

Tang, Y. and G. Mazanti (2017). "Stability analysis of coupled linear ODE-hyperbolic PDE systems with two time scales". In: *Automatica* 85, pp. 386–396. DOI: [10.1016/j.automatica.2017.07.052](https://doi.org/10.1016/j.automatica.2017.07.052).

Tang, Y., C. Prieur, and A. Girard (2015). "Tikhonov theorem for linear hyperbolic systems". In: *Automatica* 57, pp. 1–10. DOI: [10.1016/j.automatica.2015.03.028](https://doi.org/10.1016/j.automatica.2015.03.028).

Vazquez, R. and M. Krstić (2006). "Explicit integral operator feedback for local stabilization of nonlinear thermal convection loop PDEs". In: *Syst. Control Lett.* 55.8, pp. 624–632. DOI: [10.1016/j.sysconle.2005.09.019](https://doi.org/10.1016/j.sysconle.2005.09.019).

– (2007). *Control of Turbulent and Magnetohydrodynamic Channel Flows*. Boston: Birkhäuser.

Velenis, E. et al. (2005). "Dynamic tyre friction models for combined longitudinal and lateral vehicle motion". In: *Veh. Syst. Dyn.* 43.1, pp. 3–29.

Weiss, G. and R. Curtain (1997). "Dynamic stabilization of regular linear systems". In: *IEEE Trans. Autom. Control* 42.1, pp. 4–21. DOI: [10.1109/9.553684](https://doi.org/10.1109/9.553684).

Zhou, H. et al. (2018). "Coordinated Longitudinal and Lateral Motion Control for Four Wheel Independent Motor-Drive Electric Vehicle". In: *IEEE Transactions on Vehicular Technology* 67.5, pp. 3782–3790. DOI: [10.1109/TVT.2018.2816936](https://doi.org/10.1109/TVT.2018.2816936).